To appear in *Optimization Methods & Software*
Vol. 00, No. 00, Month 20XX, 1–28

RESEARCH ARTICLE

Numerical solution of optimal control problems with explicit and implicit switches

Hans Georg Bock[a], Christian Kirches[b], Andreas Meyer[a]* and Andreas Potschka[a]

[a]*Interdisciplinary Center for Scientific Computing (IWR), Heidelberg University, Germany*
[b]*Institut für Mathematische Optimierung, Technische Universität Carolo-Wilhelmina zu Braunschweig, Germany.*

(*Received 00 Month 20XX; final version received 00 Month 20XX*)

In this article, we present a unified framework for the numerical solution of optimal control problems constrained by ordinary differential equations with both implicit and explicit switches. We present the problem class and qualify different types of implicitly switched systems. This classification significantly affects opportunities for solving such problems numerically. By using techniques from generalized disjunctive programming, we transform the problem into a counterpart one wherein discontinuities no longer appear implicitly. Instead, the new problem contains discrete decision variables and vanishing constraints. Recent results from the field of mixed-integer optimal control theory enable us to omit integrality constraints on variables, and allow to solve a relaxed optimal control problem. We use a "first discretize, then optimize" approach to solve the problem numerically. A direct method based on adaptive collocation is used for the discretization. The resulting finite dimensional optimization problems are mathematical programs with vanishing constraints, and we discuss numerical techniques to solve sequences of this challenging problem class. To demonstrate the efficacy and merit of our proposed approach, we investigate three benchmark problems for hybrid dynamic systems.

Keywords: switched systems; generalized disjunctive programming; optimal control; mixed-integer optimal control; direct transcription methods; mathematical programs with vanishing constraints

1. Introduction

Switched dynamic systems, which are a particular class of hybrid dynamic systems, have been extensively researched over the past decades and a lot of progress has been made in this field of applied mathematics both theoretically and computationally, cf. [3, 19, 24, 57, 62]. In this article, we propose a new approach for solving a class of switched dynamic systems in a numerically efficient way, based on generalized disjunctive programming, a direct approach to optimal control, and on solving mathematical programs with vanishing constraints.

Hybrid systems are dynamic systems that involve continuous models as well as discrete event models. Applications of hybrid systems arise, amongst others, in the fields of industrial process control, power systems, and traffic control. Zhu and Antsaklis [62] provide a detailed survey on the topic. We give a short review on existing methods in

*Corresponding author. Im Neuenheimer Feld 205, 69120 Heidelberg, Germany. Phone: +49 (6221) 54-14610. E-mail: andreas.meyer@iwr.uni-heidelberg.de

relation to our approach.

Based on dynamic programming Branicky et al. [17] discuss necessary conditions for the existence of optimal control laws for hybrid systems. Sussmann [56] and Piccoli [47] use the maximum principle to derive necessary optimality conditions for trajectories of hybrid systems. To obtain an approximation of hybrid optimal control laws as well as upper and lower bounds of the objective value, Hedlund and Rantzer [29] use convex dynamic programming. This approach requires the state space to be discretized in order to solve the corresponding Hamilton–Jacobi–Bellmann equations and to obtain the optimal feedback control law.

In the context of this article, switched systems are optimal control problems (OCPs) with state-dependent discontinuities. In particular, all subsystems live in the same state space and there are no jumps in the states. Switched systems can be represented by an indexed set of differential equations

$$\dot{\mathbf{x}}(t) = \mathbf{F}_{\mathbf{i}(t)}(\mathbf{x}(t), \mathbf{u}(t)), \quad \mathbf{x}(t_0) = x_0. \tag{1}$$

At any point in time on the horizon $\mathcal{T} \triangleq [t_0, t_\mathrm{f}]$, a function $\mathbf{i} : \mathcal{T} \to \mathcal{M} \triangleq \{1, \ldots, M\}$ indicates the index of the applicable dynamic right hand side. Assuming that only a finite number of switching events occurs, the switching function $\mathbf{i}$ of (1) may be identified with a finite vector of tuples $s = [(\tau_0, i_0), (\tau_1, i_1), \ldots, (\tau_N, i_N)]$, where $0 \leq N < \infty$, $i_j \in \mathcal{M}$ for all $j = 0, \ldots, N$ and $t_0 = \tau_0 \leq \tau_1 \leq \ldots \leq \tau_N = t_\mathrm{f}$ Thus, the switching function is determined by the switching sequence $\sigma = \{i_j\}_{j=0}^N$ and the associated switching times $\tau = \{\tau_j\}_{j=0}^N$.

We generally distinguish two kinds of switches: *externally forced switches* (EFSs) and *internally forced switches* (IFSs). EFSs are also known as *controllable* or *explicit switches*. For problems involving EFSs the switchings are degrees of freedom. Conversely, switches in IFS problems depend on the state $\mathbf{x}$ and the current mode $\mathbf{i}$. IFS systems arise for instance from ground contact of a robot leg or from a weir overflow of a distillation column. *Implicit switch* is another well known term for IFS. Most of the literature does not address combined EFS and IFS problems. One advantage of our approach is that EFS and IFS problems are handled in a unified framework.

Most algorithms for solving EFS systems can be assigned to two kinds of methodologies: *two-stage optimization* and *embedding transformation*. Two-stage optimization algorithms work as follows: in stage 1 the switching sequence σ is assumed to be fixed and the switching times τ as well as the optimal control input $\mathbf{u}$ is optimized. In the high level stage 2 the switching sequence is updated. This process is repeatedly executed until convergence. Several authors, e.g., [25, 26, 42, 44, 59], independently employ a bi-level hierarchical algorithm to solve stage 1 and stage 2. In [45] a direct simultaneous method is used to solve the stage 1 problem. A Mixed-Integer Nonlinear Programming (MINLP) master problem updates the switching sequence. Allgor and Barton [2] and Bansal et al. [5] apply direct single shooting to the Stage 1 problem. Algorithms involving gradient projection and constrained Newton's method can be found in [60, 61].

Embedding transformation reformulates the switched dynamic system (1) into the larger family of continuous systems

$$\dot{\mathbf{x}}(t) = \sum_{i=1}^{N} \boldsymbol{\alpha}_i(t)\, \mathbf{F}_i(\mathbf{x}(t), \mathbf{u}(t)), \quad \mathbf{x}(t_0) = x_0, \tag{2}$$

where $\boldsymbol{\alpha}_i(t) \in [0,1]$ and $\sum_{i=1}^{N} \boldsymbol{\alpha}_i(t) = 1$. At the beginning of the optimization no assumptions about the number of switches, the switching sequence σ and the switching times τ are necessary. The technique of embedding transformation has been developed independently by Sager [51] and Bengea and DeCarlo [10] for EFS systems. The arising continuous OCP can be solved by standard OCP algorithms, e.g. direct multiple shooting [53] and direct collocation methods [58]. Our approach combines the ideas of complementarity based formulations for EFS systems developed by Baumrucker and Biegler [6] with the idea of embedding transformation to create a unified approach for systems with combinations of explicitly and implicitly forced switches. In addition, we would like to point out that the discretized problems belong to the subclass of Mathematical Programs with Vanishing Constraints (MPVCs), which allow for specially tailored Lagrangians and KKT conditions in contrast to the larger class of Mathematical Programs with Complementarity Constraints, a line of research that exceeds the scope of this article.

A large part of the literature dealing with IFS problems concentrates on piecewise affine (PWA) systems, e.g. [9, 33, 35, 49]. A PWA system

$$\begin{aligned} \mathbf{x}(t+1) &= A_i\,\mathbf{x}(t) + B_i\,\mathbf{u}(t) + f_i, \text{if} \\ \begin{bmatrix}\mathbf{x}(t)\\ \mathbf{u}(t)\end{bmatrix} &\in \mathcal{X}_i \triangleq \left\{ \begin{bmatrix} x \\ u \end{bmatrix} \mid G_i\,x + H_i\,u \leq K_i \right\}, \end{aligned}$$

partitions the state space into polyhedral regions $\{\mathcal{X}_i\}_{i=1}^{M}$ and associates with each region its own linear difference equation. It can be expanded by mode independent constraints

$$I\,\mathbf{x}(t) + J\,\mathbf{u}(t) \leq L.$$

Cost functions are of type

$$\mathbf{J}\left(\mathbf{u}(0),\ldots,\mathbf{u}(T-1),\mathbf{x}(0)\right) \triangleq \|P\mathbf{x}(T)\|_p \;+\; \sum_{j=0}^{T-1} \left(\|Q\mathbf{x}(j)\|_p + \|R\mathbf{u}(j)\|_p\right). \tag{3}$$

There are two types of solution strategies for PWA constrained optimization problems. One method is to embed the problems into the mixed logical dynamic (MLD) framework resulting in a system that contains a system of difference equations involving continuous as well as boolean variables. Details on MLD can be found in [8]. If we reformulate PWA problems in the MLD framework we end up either with Mixed Integer Quadratic Programs (MIQPs) when we choose $p = 2$ (see e.g., [8]) in (3) or if $p \in \{1, \infty\}$ with Mixed Integer Linear Programs (MILPs) (see e.g., [7]). A second approach to solve PWA problems was proposed in [14] and [15], where dynamic programming strategies in combination with multi-parametric program solvers are applied.

More general IFS OCPs are often solved by combining a modern simultaneous optimization method (e.g., direct multiple shooting [13]) with an appropriate switch detecting differential equation solver (see e.g., [12, 16, 36]). The main challenges of switch detecting solvers are the determination of the switching time and the sensitivity update process at discontinuities (see e.g., [16, 30, 36, 39, 50]). Models where both the number and the sequence of arising switching points are known can be handled by multi-phase OCPs (see e.g., [46, 55]). In this case the implicit discontinuities do not have to be treated explicitly.

1.1 *Contributions*

OCPs constrained by ordinary differential equations with implicitly defined, state-dependent discontinuities are notoriously difficult to solve. This is particularly true if a combination of explicit and inconsistent switching behavior is present in the solution. We propose a novel method to solve such problems in a unified way by establishing a counterpart formulation in terms of binary indicator functions. Our approach is based on an idea from generalized disjunctive programming, and on a direct and simultaneous approach to optimal control. We apply recent results from the field of mixed-integer optimal control theory that enable us to omit integrality constraints on variables. As a result, we obtain a sequence of adaptively refined MPVCs that may be solved using highly performant codes for nonlinear programming. We demonstrate the efficacy and merit of our proposed approach by investigating three benchmark problems for hybrid dynamic systems.

1.2 *Structure of the Article*

This article is organized as follows: In Section 2, we formulate a broad class of switched OCPs and discuss aspects of switched systems possibly leading to numerical difficulties. By means of the general disjunctive programming framework we convert the implicitly switched system into an explicit one subject to additional constraints and boolean control variables. Recent results enable us to relax the integrality condition, as the relaxed problem yields an objective value that can be reached by boolean control functions up to any given accuracy threshold, cf. [22, 28, 37, 51]. Section 3 uses a direct transcription method to transfer the relaxed continuous OCP into a mathematical program with vanishing constraints. Section 4 deals with the numerical issues of solving this special type of nonlinear programming problems (NLPs). Numerical experiments in Section 5 demonstrate the reliability of our approach.

2. Problem Formulation

In this section we first describe the transformation of an implicitly switched OCP to a mixed-integer optimal control problem (MIOCP) by introducing additional boolean control variables and vanishing constraints. In a second step we show how recent results enable us to replace this difficult problem by a relaxed version without loosing integrality.

2.1 *Optimal Control Problems with explicit and implicit Switches*

In this article, we consider the explicitly and implicitly Switched Optimal Control Problem (SOCP)

$$
\begin{aligned}
\min_{\mathbf{x}(\cdot),\mathbf{u}(\cdot),\mathbf{w}(\cdot)} \quad & \phi(\mathbf{x}(t_\mathrm{f})) \\
\text{s.t.} \quad & \dot{\mathbf{x}}(t) = \hat{\mathbf{f}}(\mathbf{x}(t),\mathbf{u}(t),\mathbf{w}(t),\operatorname{sgn}(\boldsymbol{\sigma}(t,\mathbf{x}(t)))), && t\in\mathcal{T}, \\
& 0 \geq \mathbf{c}(\mathbf{x}(t),\mathbf{u}(t)), && t\in\mathcal{T}, \\
& 0 \geq \mathbf{r}(\mathbf{x}(t_0),\mathbf{x}(t_\mathrm{f})), \\
& \mathbf{w}(t) \in \mathcal{W} = \{W_1,\ldots,W_{n_\mathrm{w}}\},
\end{aligned}
\tag{SOCP}
$$

$$
\tag{4}
$$

where the dynamic process $\mathbf{x} : \mathcal{T} \to \mathcal{X}$ is determined by a dynamical system with right hand side function $\hat{\mathbf{f}} : \mathcal{X} \times \mathcal{U} \times \mathcal{W} \times \{-1, 0, +1\}^{n_\sigma} \to \mathbb{R}^{n_\mathrm{x}}$, affected by continuously-valued control function $\mathbf{u} : \mathcal{T} \to \mathcal{U}$ and a discretely-valued control function $\mathbf{w} : \mathcal{T} \to \mathcal{W}$ on a time horizon $\mathcal{T} \triangleq [t_0, t_\mathrm{f}] \subset \mathbb{R}$, such that a Mayer type performance index $\phi : \mathcal{X} \to \mathbb{R}$ is minimized. Path constraints $\mathbf{c} : \mathcal{X} \times \mathcal{U} \to \mathbb{R}^{n_\mathrm{c}}$ and point constraints $\mathbf{r} : \mathcal{X} \times \mathcal{X} \to \mathbb{R}^{n_\mathrm{r}}$ must be satisfied. Implicitly forced discontinuities of $\hat{\mathbf{f}}$ are determined by the sign structure of the switch function $\boldsymbol{\sigma} : \mathcal{T} \times \mathcal{X} \to \mathbb{R}^{n_\sigma}$. The function $\boldsymbol{\sigma}$ is assumed to be a $\mathcal{C}^1$ function of time t and state $\mathbf{x}$.

The set $\mathcal{X} = \mathbb{R}^{n_\mathrm{x}}$ denotes the range of the states, the set $\mathcal{U} = \mathbb{R}^{n_\mathrm{u}}$ the range of the continuously-valued controls, and the set $\mathcal{W} \subset \mathbb{R}^{n_\mathrm{w}}$ the finite range of the discretely-valued controls. The functions ϕ, $\hat{\mathbf{f}}$, $\mathbf{c}$, and $\mathbf{r}$ are assumed to be $\mathcal{C}^2$ functions of their arguments.

The function $\mathbf{r}$ allows the definition of initial and terminal constraints. We assume the switch function $\boldsymbol{\sigma}$ to be one dimensional, i.e. $n_\sigma = 1$. This makes notations easier for the rest of this section. At appropriate places we will outline the extension to higher dimensions. We restrict ourselves to objectives of Mayer type. All other types may be regarded as additional differential states evaluated at final time contributing to the objective of Mayer type. The formulation of (SOCP) as an autonomous system does not limit the problem class because every non-autonomous system can be transformed into an autonomous one by introducing an additional state.

2.2 *Consistent Switches*

The sign structure of $\boldsymbol{\sigma}$ in the right hand side function $\hat{\mathbf{f}}$ of the dynamic system (SOCP) yields a non-differentiability in the dynamics. This coincides with our definition of a switched system (1). If $\boldsymbol{\sigma}$ is independent of $\mathbf{x}$ the switch is an EFS or explicit switch. Otherwise the switch is an IFS or implicit switch. An activation time $t_\mathrm{s} \in \mathcal{T}$ of the switch is implicitly defined by a zero-crossing of $\boldsymbol{\sigma}$. The sign structure of $\boldsymbol{\sigma}$ uniquely identifies the activation state of the switch.

For a detailed discussion of implicit switches we introduce some notation. At a switching point $t_\mathrm{s} \in \mathcal{T}$, the left and right hand side limits of the dynamic process $\mathbf{x}$ are defined as

$$\mathbf{x}^-(t_\mathrm{s}) \triangleq \lim_{t \nearrow t_\mathrm{s}} \mathbf{x}(t), \quad \mathbf{x}^+(t_\mathrm{s}) \triangleq \lim_{t \searrow t_\mathrm{s}} \mathbf{x}(t).$$

The one-sided derivatives

$$\mathcal{D}\boldsymbol{\sigma}^-(t_\mathrm{s}) \triangleq \frac{\mathrm{d}\boldsymbol{\sigma}}{\mathrm{d}t}(t_\mathrm{s}, \mathbf{x}^-(t_\mathrm{s})), \quad \mathcal{D}\boldsymbol{\sigma}^+(t_\mathrm{s}) \triangleq \frac{\mathrm{d}\boldsymbol{\sigma}}{\mathrm{d}t}(t_\mathrm{s}, \mathbf{x}^+(t_\mathrm{s}))$$

of $\boldsymbol{\sigma}$ at the switching point t_s allow for a qualification of the switch, as follows.

A large class of switched dynamic systems satisfies the *transversality assumption*. Such systems permit solutions that cross the zero manifold

$$\Sigma \triangleq \{(t, \mathbf{x}) \in \mathcal{T} \times \mathbb{R}^{n_\mathrm{x}} \mid \boldsymbol{\sigma}(t, \mathbf{x}) = 0\}$$

in either direction. Hence, a finite number of isolated switching events occurs on a finite time horizon. Such solutions are often referred to as "classical", and the switching behavior is often called "consistent".

ASSUMPTION 2.1 (Transversality) *Problem* (SOCP) *satisfies the* transversality *assumption if* $\mathcal{D}\boldsymbol{\sigma}^-(t_\mathrm{s}) \cdot \mathcal{D}\boldsymbol{\sigma}^+(t_\mathrm{s}) > 0$ *for all* $t_\mathrm{s} \in \mathcal{T}$ *with* $\sigma(t_\mathrm{s}) = 0$.

If the transversality assumption holds, only finitely many isolated points of the zero manifold Σ are part of a solution trajectory $\mathbf{x}$. We may then skip over the case $\boldsymbol{\sigma} = 0$ and the problem becomes easier to formulate and to solve numerically. Our method is a promising candidate for the unified solution of the more difficult case when $\boldsymbol{\sigma}(t, \mathbf{x}(t)) = 0$ holds on a proper interval $[t_\mathrm{s}, t^+] \subset \mathcal{T}$, which we discuss next.

2.3 *Inconsistent Switches and Filippov Solutions*

If $\mathcal{D}\boldsymbol{\sigma}^-(t_\mathrm{s}) \cdot \mathcal{D}\boldsymbol{\sigma}^+(t_\mathrm{s}) \leq 0$, the transversality Assumption 2.1 is violated and one distinguishes several so-called "non-classical" cases.

First, if $\mathcal{D}\boldsymbol{\sigma}^-(t_\mathrm{s}) > 0$ and $\mathcal{D}\boldsymbol{\sigma}^+(t_\mathrm{s}) < 0$, the switch indicates a bifurcation location and the zero manifold Σ could be left in either direction, which cannot be determined from the dynamics of the system alone. Within a control problem, one direction might be preferable to the other. We do not consider this difficult case further in this paper.

If $\mathcal{D}\boldsymbol{\sigma}^-(t_\mathrm{s}) < 0$ and $\mathcal{D}\boldsymbol{\sigma}^+(t_\mathrm{s}) > 0$, the zero manifold cannot be left and the switch is often called an "inconsistent" switch. A continuation on the manifold Σ in the sense of Filippov [20] may be found by replacing $\hat{\mathbf{f}}$ in (SOCP) by an appropriate linear combination

$$\hat{\mathbf{f}}_\alpha(\mathbf{x}(t), \mathbf{u}(t)) := \alpha(t)\hat{\mathbf{f}}(\mathbf{x}(t), \mathbf{u}(t), -1) + (1 - \alpha(t))\hat{\mathbf{f}}(\mathbf{x}(t), \mathbf{u}(t), +1), \quad \alpha(t) \in (0, 1),$$

that satisfies $\sigma(t, \mathbf{x}(t)) = 0$ for all $t \in [t_\mathrm{s}, t^+]$. Here $t^+ > t_\mathrm{s}$ is a later time point with switching function derivatives that permit leaving the manifold. We elaborate on the tight connection of the embedding transformation approach (2) with Filippov solutions below. A completely automatic computation of Filippov solutions is beyond the scope of this article and left for further studies. We highlight the major challenges that need to be mastered to that end in Section 6.

If one of first order derivatives $\mathcal{D}\boldsymbol{\sigma}^+$ or $\mathcal{D}\boldsymbol{\sigma}^-$ vanishes, the state trajectory tangentially enters or leaves the zero manifold Σ. Higher-order derivatives of the switching function $\boldsymbol{\sigma}$ would have to be analyzed to learn the type of continuation. The derivation of suitable problem formulations and an implementation of a numerical code that addresses this situation is also left to future research.

Finally, a remark on optimal control problems with solutions that switch infinitely often on a finite time horizon, sometimes called "chattering" behavior, is appropriate. In this article, we pursue a direct approach to optimal control, which relies on a discretization of the control in time. Hence, any computable optimal solution will necessarily approximate such a solution using only a finite number of switches. We make use of a collocation mesh refinement device near time points where switches occur, which increases the number of *potential* switching locations. After refinement and re-optimization, this will give an indication of whether or not the number of *actual* switches of the optimal solutions of the discretized problems increases with the mesh resolution. All computational examples in this article possess optimal solutions with a finite number of switches.

ASSUMPTION 2.2 *Problem* (SOCP) *permits optimal solutions with a finite number of switches.*

2.4 *Optimal Control of Hybrid Systems*

In this section problem (SOCP) is reformulated in the sense of a hybrid OCP using an indexed set of differential equations as done in (1). According to the observations of the previous section we distinguish two cases: if the transversality Assumption 2.1 holds (consistent switching) we can equivalently rewrite (SOCP) as

$$\begin{aligned} \min_{\mathbf{x}(\cdot),\mathbf{u}(\cdot),\mathbf{w}(\cdot)} \quad & \phi(\mathbf{x}(t_\mathrm{f})) \\ \text{s.t.} \quad & \dot{\mathbf{x}}(t) = \begin{cases} \mathbf{f}^+(\mathbf{x}(t),\mathbf{u}(t),\mathbf{w}(t)) & \text{if } \boldsymbol{\sigma}(t,\mathbf{x}(t)) \geq 0, \\ \mathbf{f}^-(\mathbf{x}(t),\mathbf{u}(t),\mathbf{w}(t)) & \text{if } \boldsymbol{\sigma}(t,\mathbf{x}(t)) \leq 0, \end{cases} && t \in \mathcal{T}, \\ & 0 \geq \mathbf{c}(\mathbf{x}(t),\mathbf{u}(t)), && t \in \mathcal{T}, \\ & 0 \geq \mathbf{r}(\mathbf{x}(t_0),\mathbf{x}(t_\mathrm{f})), \\ & \mathbf{w}(t) \in \mathcal{W}, && t \in \mathcal{T}, \end{aligned} \tag{5}$$

where the functions $\mathbf{f}^+ : \mathcal{X} \times \mathcal{U} \times \mathcal{W} \to \mathbb{R}^{n_\mathrm{x}}$ and $\mathbf{f}^- : \mathcal{X} \times \mathcal{U} \times \mathcal{W} \to \mathbb{R}^{n_\mathrm{x}}$ are chosen appropriately. If the transversality assumption is violated (inconsistent switching), we additionally have to consider the Filippov case of sliding on the zero manifold Σ:

$$\begin{aligned} \min_{\mathbf{x}(\cdot),\mathbf{u}(\cdot),\mathbf{w}(\cdot)} \quad & \phi(\mathbf{x}(t_\mathrm{f})) \\ \text{s.t.} \quad & \dot{\mathbf{x}}(t) = \begin{cases} \mathbf{f}^+(\mathbf{x}(t),\mathbf{u}(t),\mathbf{w}(t)) & \text{if } \boldsymbol{\sigma}(t,\mathbf{x}(t)) > 0, \\ \mathbf{f}^-(\mathbf{x}(t),\mathbf{u}(t),\mathbf{w}(t)) & \text{if } \boldsymbol{\sigma}(t,\mathbf{x}(t)) < 0, \\ \mathbf{f}^0(\mathbf{x}(t),\mathbf{u}(t),\mathbf{w}(t)) & \text{if } \boldsymbol{\sigma}(t,\mathbf{x}(t)) = 0, \end{cases} && t \in \mathcal{T}, \\ & 0 \geq \mathbf{c}(\mathbf{x}(t),\mathbf{u}(t)), && t \in \mathcal{T}, \\ & 0 \geq \mathbf{r}(\mathbf{x}(t_0),\mathbf{x}(t_\mathrm{f})), \\ & \mathbf{w}(t) \in \mathcal{W}, && t \in \mathcal{T}. \end{aligned} \tag{6}$$

The dynamics for the latter case are denoted by $\mathbf{f}^0 : \mathcal{X} \times \mathcal{U} \times \mathcal{W} \to \mathbb{R}^{n_\mathrm{x}}$. The objective function ϕ and the constraint functions $\mathbf{c}$, $\mathbf{r}$ do not change in (5) and (6). For $n_\sigma > 1$ we would obtain 2^{n_σ} cases for consistent switches in the worst case. If the transversality assumption does not hold for any switch, there could be as many as 3^{n_σ}. Usually, however, not all components of $\hat{\mathbf{f}}$ depend on all switches, and a much better complexity is observed during reformulation.

An approach very close in spirit was described by Baumrucker and Biegler [6]. Note, however, that our approach does not reformulate the original ordinary differential equation with discontinuous right hand side into a differential algebraic equation on intervals with $\boldsymbol{\sigma} \equiv 0$, but rather leaves the resolution of the sliding mode right hand side to the choice of the convex multipliers within the optimizer.

2.5 *Generalized Disjunctive Programming*

Optimization problems involving both continuous and discrete variables are often solved with techniques from mixed-integer optimization. Disjunctive Programming (DP) is an alternative approach to solve these kind of problems, see e.g. [4]. DP models consist of algebraic constraints, logic disjunctions and logic propositions. A particular case of disjunctive programming named Generalized Disjunctive Programming (GDP) was de-

veloped by Raman and Grossmann [48]. A GDP problem reads as

$$\begin{aligned}
\min_{x\in\mathbb{R}^n,\,\omega_{ik}\in\{0,1\}} \quad & \psi(x)+\sum_{k\in K} c_k,\\
\text{s.t.} \quad & \mathbf{g}(x)\le 0,\\
& \bigoplus_{i\in\mathcal{D}_k}\begin{bmatrix}\omega_{ik}=1\\ \mathbf{s}_{ik}(x)\le 0\\ c_k=\gamma_{ik}\end{bmatrix}, \qquad k\in\mathcal{K}\triangleq\{1,\dots,K\},\ \mathcal{D}_k\triangleq\{1,\dots,D_k\},\\
& \Omega(\omega)=1,\\
& x\in[x^{\mathrm{l}},x^{\mathrm{u}}].
\end{aligned}$$

The problem involves continuous variables $x\in\mathbb{R}^n$ in the bounds $[x^{\mathrm{l}},x^{\mathrm{u}}]$ and binary variables $\omega\triangleq\{\omega_{ik}\}_{i,k}$, $\omega_{ik}\in\{0,1\}$. The objective function $\psi:\mathbb{R}^n\to\mathbb{R}$ and the global constraint function $\mathbf{s}:\mathbb{R}^n\to\mathbb{R}^m$ are supposed to be sufficiently smooth. K logical expression must hold. Each of these expressions is composed of D_k terms that are connected by the EX-OR operator $\oplus$, indicating that exactly one of the boolean variables w_{ik} must be set to one. If that is the case for a particular variable w_{ik}, the associated constraint $\mathbf{s}_{ik}(x)\le 0$ and the objective weight c_k are enforced. They are ignored for all $\omega_{ik}=0$. The constraint $\Omega(\omega)=1$ summarizes further constraints on the boolean variables ω_{ik}.

By reformulating problem (6) in the GDP framework, we obtain the equivalent problem

$$\begin{aligned}
\min_{\mathbf{x}(\cdot),\,\mathbf{u}(\cdot),\,\boldsymbol{\omega}(\cdot)} \quad & \phi(\mathbf{x}(t_{\mathrm{f}}))\\
\text{s.t.} \quad & \bigoplus_{w\in\mathcal{W}}\left[\begin{array}{c|c|c}\boldsymbol{\omega}_+^w(t)=1 & \boldsymbol{\omega}_-^w(t)=1 & \boldsymbol{\omega}_0^w(t)=1\\ \dot{\mathbf{x}}(t)=\mathbf{f}^+(\mathbf{x}(t),\mathbf{u}(t),w) & \dot{\mathbf{x}}(t)=\mathbf{f}^-(\mathbf{x}(t),\mathbf{u}(t),w) & \dot{\mathbf{x}}(t)=\mathbf{f}^0(\mathbf{x}(t),\mathbf{u}(t),w)\\ \boldsymbol{\sigma}(t,\mathbf{x}(t))>0 & \boldsymbol{\sigma}(t,\mathbf{x}(t)<0 & \boldsymbol{\sigma}(t,\mathbf{x}(t))=0\end{array}\right],\\
& 0\ge\mathbf{c}(\mathbf{x}(t),\mathbf{u}(t)),\quad t\in\mathcal{T},\\
& 0\ge\mathbf{r}(\mathbf{x}(t_0),\mathbf{x}(t_{\mathrm{f}})),
\end{aligned}\tag{7}$$

where the disjunction over all three clauses in the brackets and all explicitly switchable modes in $\mathcal{W}$ must hold at any point $t\in\mathcal{T}$ and the objective function ϕ and the global constraints $\mathbf{c}$ and $\mathbf{r}$ do not depend on the explicitly and implicitly switched mode. The equivalent reformulation of problem (6) to problem (7) is crucial because it transforms an implicitly switched system into an explicit one by introducing additional boolean control variables and constraints and therefore unifies the treatment of explicit and implicit switches.

Formulation (7) is ill-posed in a computational setting, as it is numerically difficult to distinguish between the equality and the two inequality cases. For consistently switched systems we can set $\varepsilon\equiv 0$, introduce the tractable constraints $\boldsymbol{\sigma}(t,\mathbf{x}(t))\ge 0$ and $\boldsymbol{\sigma}(t,\mathbf{x}(t))\le 0$ for the first two modes, respectively, and dispose of the third mode. For inconsistently switched systems, one avenue to handling the arising numerical issues is

to introduce an ε-tube for the case $\boldsymbol{\omega}_0(t) = 1$, as follows:

$$\begin{aligned}
\min_{\mathbf{x}(\cdot),\,\mathbf{u}(\cdot),\,\boldsymbol{\omega}(\cdot)}\ & \phi(\mathbf{x}(t_\mathrm{f})) \\
\text{s.t.}\ & \bigoplus_{w\in\mathcal{W}} \left[\begin{array}{c|c|c} \boldsymbol{\omega}_+^w(t) = 1 & \boldsymbol{\omega}_-^w(t) = 1 & \boldsymbol{\omega}_0^w(t) = 1 \\ \dot{\mathbf{x}}(t) = \mathbf{f}^+(\mathbf{x}(t),\mathbf{u}(t),w) & \dot{\mathbf{x}}(t) = \mathbf{f}^-(\mathbf{x}(t),\mathbf{u}(t),w) & \dot{\mathbf{x}}(t) = \mathbf{f}^0(\mathbf{x}(t),\mathbf{u}(t),w) \\ \boldsymbol{\sigma}(t,\mathbf{x}(t)) \geq +\varepsilon & \boldsymbol{\sigma}(t,\mathbf{x}(t)) \leq -\varepsilon & -\varepsilon \leq \boldsymbol{\sigma}(t,\mathbf{x}(t)) \leq +\varepsilon \end{array}\right], \\
& 0 \geq \mathbf{c}(\mathbf{x}(t),\mathbf{u}(t)), \quad t\in\mathcal{T}, \\
& 0 \geq \mathbf{r}(\mathbf{x}(t_0),\mathbf{x}(t_\mathrm{f})).
\end{aligned} \tag{8}$$

In some practical problems, function $\mathbf{f}^0$ may be a linear combination of $\mathbf{f}^+$ and $\mathbf{f}^-$, leading to redundancies in the constraint set formulation. Moreover, such a linear combination may be state dependent and of Filippov type, and it will be desirable for a computational approach to identify it automatically. To rid the formulation of constraint redundancy, we may then wish to solve the following GDP problem instead of problem (8):

$$\begin{aligned}
\min_{\mathbf{x}(\cdot),\,\mathbf{u}(\cdot),\,\boldsymbol{\omega}(\cdot)}\ & \phi(\mathbf{x}(t_\mathrm{f})) \\
\text{s.t.}\ & \bigoplus_{w\in\mathcal{W}} \left[\begin{array}{c|c} \boldsymbol{\omega}_+^w(t) = 1 & \boldsymbol{\omega}_-^w(t) = 1 \\ \dot{\mathbf{x}}(t) = \mathbf{f}^+(\mathbf{x}(t),\mathbf{u}(t),w) & \dot{\mathbf{x}}(t) = \mathbf{f}^-(\mathbf{x}(t),\mathbf{u}(t),w) \\ \boldsymbol{\sigma}(t,\mathbf{x}(t)) \geq -\varepsilon & \boldsymbol{\sigma}(t,\mathbf{x}(t)) \leq +\varepsilon \end{array}\right], \quad t\in\mathcal{T}, \\
& 0 \geq \mathbf{c}(\mathbf{x}(t),\mathbf{u}(t)), \qquad\qquad t\in\mathcal{T}, \\
& 0 \geq \mathbf{r}(\mathbf{x}(t_0),\mathbf{x}(t_\mathrm{f})).
\end{aligned} \tag{9}$$

Here, the ε-tubes of either mode overlap, and both modes are feasible on subarcs showing inconsistent switching behavior. We return to the advantages of this formulation when discussing a particular relaxation in the next section.

2.6 *Mixed Integer Optimal Control Problems*

In this section, we apply a technique from [34, 37, 38] that makes use of mathematical programs with vanishing constraints, cf. [1, 31], to obtain a constraint formulation for the disjunction in the GDP problems (7–9) that is amenable to the direct approach to optimal control. Problem (7) can be equivalently reformulated as a MIOCP

$$\begin{aligned}
\min_{\mathbf{x}(\cdot),\,\mathbf{u}(\cdot),\,\boldsymbol{\omega}(\cdot)}\ & \phi(\mathbf{x}(t_\mathrm{f})) \\
\text{s.t.}\ & \dot{\mathbf{x}}(t) = \mathbf{f}(\mathbf{x}(t),\mathbf{u}(t),\boldsymbol{\omega}(t)) \triangleq \sum_{\substack{w\in\mathcal{W},\\ i\in\{-,0,+\}}} \boldsymbol{\omega}_i^w(t)\,\mathbf{f}^i(\mathbf{x}(t),\mathbf{u}(t),w), && t\in\mathcal{T}, \\
& 0 \geq \mathbf{c}(\mathbf{x}(t),\mathbf{u}(t)), && t\in\mathcal{T}, \\
& 0 \geq \mathbf{r}(\mathbf{x}(t_0),\mathbf{x}(t_\mathrm{f})), \\
& 0 \geq -\boldsymbol{\omega}_+^w(t)\,(\boldsymbol{\sigma}(t,\mathbf{x}(t)) - \varepsilon), && w\in\mathcal{W},\ t\in\mathcal{T}, \\
& 0 \geq +\boldsymbol{\omega}_-^w(t)\,(\boldsymbol{\sigma}(t,\mathbf{x}(t)) + \varepsilon), && w\in\mathcal{W},\ t\in\mathcal{T}, \\
& 0 \geq +\boldsymbol{\omega}_0^w(t)\,(\boldsymbol{\sigma}(t,\mathbf{x}(t)) - \varepsilon), && w\in\mathcal{W},\ t\in\mathcal{T}, \\
& 0 \geq -\boldsymbol{\omega}_0^w(t)\,(\boldsymbol{\sigma}(t,\mathbf{x}(t)) + \varepsilon), && w\in\mathcal{W},\ t\in\mathcal{T}, \\
& \boldsymbol{\omega}(t) \in \mathbb{S}^{3^{n_\mathrm{w}}}, && t\in\mathcal{T}.
\end{aligned} \tag{10}$$

To guarantee that exactly one term in the disjunction is active, we define the set

$$\mathbb{S}^{3^{n_\mathrm{w}}} \triangleq \left\{ \omega_i^w \in \{0,1\},\ w \in \mathcal{W}, i \in \{-,0,+\} \mid \sum\nolimits_{w\in\mathcal{W}, j\in\{-,0,+\}} \omega_j^w = 1 \right\}$$

of all vectors $\boldsymbol{\omega} \triangleq [\omega_-^{W_1}, \omega_0^{W_1}, \omega_+^{W_1}, \ldots, \omega_-^{W_{n_\mathrm{w}}}, \omega_0^{W_{n_\mathrm{w}}}, \omega_+^{W_{n_\mathrm{w}}}]^T$ with the *special ordered set type 1 (SOS1) property*. We obtain a relaxed counterpart problem for (10) by relaxing the binary constraint $\boldsymbol{\omega}(t) \in \mathbb{S}^{3^{n_\mathrm{w}}}$ to the convex hull $\boldsymbol{\alpha}(t) \in \mathrm{conv}(\mathbb{S}^{3^{n_\mathrm{w}}})$:

$$\begin{aligned}
\min_{\mathbf{x}(\cdot),\,\mathbf{u}(\cdot),\,\boldsymbol{\alpha}(\cdot)} \quad & \phi(\mathbf{x}(t_\mathrm{f})) \\
\text{s.t.} \quad & \dot{\mathbf{x}}(t) = \mathbf{f}(\mathbf{x}(t), \mathbf{u}(t), \boldsymbol{\alpha}(t)), && t \in \mathcal{T}, \\
& 0 \geq \mathbf{c}(\mathbf{x}(t), \mathbf{u}(t)), && t \in \mathcal{T}, \\
& 0 \geq \mathbf{r}(\mathbf{x}(t_0), \mathbf{x}(t_\mathrm{f})), \\
& 0 \geq -\boldsymbol{\alpha}_+^w(t)\,(\boldsymbol{\sigma}(t, \mathbf{x}(t)) - \varepsilon), w \in W, && t \in \mathcal{T}, && \text{(11a)} \\
& 0 \geq +\boldsymbol{\alpha}_-^w(t)\,(\boldsymbol{\sigma}(t, \mathbf{x}(t)) + \varepsilon), w \in W, && t \in \mathcal{T}, && \text{(11b)} \\
& 0 \geq +\boldsymbol{\alpha}_0^w(t)\,(\boldsymbol{\sigma}(t, \mathbf{x}(t)) - \varepsilon), w \in W, && t \in \mathcal{T}, && \text{(11c)} \\
& 0 \geq -\boldsymbol{\alpha}_0^w(t)\,(\boldsymbol{\sigma}(t, \mathbf{x}(t)) + \varepsilon), w \in W, && t \in \mathcal{T}, && \text{(11d)} \\
& \boldsymbol{\alpha}(t) \in \mathrm{conv}(\mathbb{S}^{3^{n_\mathrm{w}}}), && t \in \mathcal{T}.
\end{aligned}$$

Problem (11) is an OCP with *vanishing constraints*. The terminology is due to the fact that the implied constraint constraint $\boldsymbol{\sigma}(t, \mathbf{x}(t)) \geq \varepsilon$ in (11a) *vanishes* as soon as $\boldsymbol{\alpha}_+(t) = 0$. Similar arguments apply to constraints (11b–11d).

Problem (11) has a larger feasible set than the original problem (10) we intended to solve. Hence, lower optimal objective function values may be attained for problem (11), and the relation of both objective function values is of interest. The following theorem gives an approximation result before discretization in time.

THEOREM 2.3 *Let $\hat{\mathbf{x}} : \mathcal{T} \to \mathbb{R}^{n_\mathrm{x}}$, $\hat{\mathbf{u}} : \mathcal{T} \to \mathbb{R}^{n_\mathrm{u}}$ and $\hat{\boldsymbol{\alpha}} : \mathcal{T} \to \mathbb{R}^{3^{n_\mathrm{w}}}$ be feasible for problem (11). Then, for every $\delta > 0$ there is $\mathbf{x}^\delta : \mathcal{T} \to \mathbb{R}^{n_\mathrm{x}}$ and $\boldsymbol{\omega}^\delta : \mathcal{T} \to \mathbb{R}^{3^{n_\mathrm{w}}}$ such that*

$$|\phi(\mathbf{x}^\delta(t_\mathrm{f})) - \phi(\hat{\mathbf{x}}(t_\mathrm{f}))| < \delta$$

and

$$\begin{aligned}
& \dot{\mathbf{x}}^\delta(t) = \mathbf{f}(\mathbf{x}^\delta(t), \hat{\mathbf{u}}(t), \boldsymbol{\omega}^\delta(t)), && t \in \mathcal{T}, \\
& \delta L_\mathrm{c} \mathbf{1} \geq \mathbf{c}(\mathbf{x}^\delta(t), \hat{\mathbf{u}}(t)), && t \in \mathcal{T}, \\
& \delta L_\mathrm{r} \mathbf{1} \geq \mathbf{r}(\mathbf{x}^\delta(t_0), \mathbf{x}^\delta(t_\mathrm{f})), \\
& \delta L_\sigma \geq -(\boldsymbol{\omega}^\delta)_+^w(t)\,(\boldsymbol{\sigma}(t, \mathbf{x}(t)) - \varepsilon), w \in W, && t \in \mathcal{T}, \\
& \delta L_\sigma \geq +(\boldsymbol{\omega}^\delta)_-^w(t)\,(\boldsymbol{\sigma}(t, \mathbf{x}(t)) + \varepsilon), w \in W, && t \in \mathcal{T}, \\
& \delta L_\sigma \geq +(\boldsymbol{\omega}^\delta)_0^w(t)\,(\boldsymbol{\sigma}(t, \mathbf{x}(t)) - \varepsilon), w \in W, && t \in \mathcal{T}, \\
& \delta L_\sigma \geq -(\boldsymbol{\omega}^\delta)_0^w(t)\,(\boldsymbol{\sigma}(t, \mathbf{x}(t)) + \varepsilon), w \in W, && t \in \mathcal{T}, \\
& \boldsymbol{\omega}^\delta(t) \in \mathbb{S}^3, && t \in \mathcal{T},
\end{aligned}$$

where L_c, L_r, and L_σ are δ-independent Lipschitz constants of the corresponding functions with respect to the state $\mathbf{x}$, and $\mathbf{1}$ denotes the suitable all-ones vector.

That is, $(\mathbf{x}^\delta, \boldsymbol{\omega}^\delta)$ is feasible for problem (10) with the exception of the (vanishing) constraints, which are violated by less than δ times a constant.

A proof of Theorem 2.3 can be found in [37], and the case of no vanishing constraints in [52, 53]. According to this theorem, every feasible point $\boldsymbol{\alpha}$ of the relaxed problem (11) can be approximated arbitrarily well by a binary feasible point $\boldsymbol{\omega}$. In particular, this approximation result also applies to optimal solutions of the relaxed counterpart problem. Note that the binary feasible point $(\mathbf{x}^\delta, \boldsymbol{\omega}^\delta)$ obtained by Theorem 2.3 in general depends on the chosen tolerance $\delta > 0$. A constructive algorithm for retrieving binary feasible controls $\boldsymbol{\omega}^\delta$ with guaranteed approximation properties is given in [37], based on [51].

3. Discretization of the Infinite Dimensional OCP

For solving the infinite dimensional OCP (11) we apply a first discretize then optimize approach. Direct transcription methods like Direct Multiple Shooting [13] and Direct Collocation [11] have been established as the methods of choice. Collocation methods transcribe the OCP to an NLP by parameterizing the states and controls using global polynomials and collocating the differential equations using nodes obtained from a Gaussian quadrature. In this contribution we choose piecewise polynomials over finite elements to discretize states and controls. Approximations of the differential states $\mathbf{x}$ are required to be $\mathcal{C}^0$ over the complete horizon $\mathcal{T}$.
We split up the horizon $\mathcal{T} = [t_0, t_\mathrm{f}]$ into $N \in \mathbb{N}$ finite elements by choosing a time grid

$$t_0 < t_1 < \cdots < t_N = t_\mathrm{f}.$$

For each finite element we choose Lagrange basis polynomials $\left\{\mathcal{L}_j^{(n)}\right\}_{j=0}^{K_n}$ and $\left\{\bar{\mathcal{L}}_j^{(n)}\right\}_{j=1}^{\bar{K}_n}$ given by

$$\mathcal{L}_j^{(n)}(t) \triangleq \prod_{\substack{i=0 \\ i\neq j}}^{K_n} \frac{t - t_i^{(n)}}{t_j^{(n)} - t_i^{(n)}}, \quad \bar{\mathcal{L}}_j^{(n)}(t) \triangleq \prod_{\substack{i=1 \\ i\neq j}}^{\bar{K}_n} \frac{t - \bar{t}_i^{(n)}}{\bar{t}_j^{(n)} - \bar{t}_i^{(n)}}, \quad n = 1, \ldots, N.$$

Depending of the concrete method the *collocation points* $t_i^{(n)}, \bar{t}_j^{(n)} \in \mathbb{R}$ $(i = 1, \ldots, K_n,\ j = 1, \ldots, \bar{K}_n,\ n = 1, \ldots, N)$ are obtained from the roots of an orthogonal polynomial and/or linear combinations of the polynomial and its derivatives. Due to their good computational efficiency (see e.g., [21, 32]) we choose flipped Legendre–Gauss–Radau (LGR) points in this contribution. If l is the number of collocation points and $\mathcal{P}_l$ denotes the l^{th}-degree Legendre polynomial LGR points are the roots of $\mathcal{P}_{l-1}(\tau) + \mathcal{P}_l(\tau)$. LGR points lie on the half open interval $t \in [-1, 1)$. One obtains the flipped LGR points by flipping the LGR points about the origin. The affine transformations

$$t^{(n)}(\tau) \triangleq \frac{t_n + t_{n-1}}{2} + \tau\ \frac{t_n - t_{n-1}}{2}, \quad n = 1, \ldots, N,$$

map flipped LGR points to the finite element intervals $\mathcal{T}_n \triangleq [t_{n-1}, t_n]$ and yield the collocation points $t_i^{(n)},\ \bar{t}_j^{(n)}$. In addition we set $t_0^{(n)} = t_{n-1}$.

The differential states are approximated element-wise as

$$\mathbf{X}(t) \triangleq \sum_{j=0}^{K_n} x_j^{(n)} \mathcal{L}_j^{(n)}(t), \quad t \in \mathcal{T}_n, \quad n = 1, \ldots, N,$$

where K_n is the number of collocation points and $x_j^{(n)} \in \mathbb{R}^{n_\mathrm{x}}$ the nodal values. The derivative with respect to the time of the differential state approximation is given by

$$\dot{\mathbf{X}}(t) = \sum_{j=0}^{K_n} x_j^{(n)} \dot{\mathcal{L}}_j^{(n)}(t), \quad t \in \mathcal{T}_n, \quad n = 1, \ldots, N.$$

Analogously to the state approximations the controls $\mathbf{u}$ are approximated by

$$\mathbf{U}(t) \triangleq \sum_{j=1}^{\bar{K}_n} u_j^{(n)} \bar{\mathcal{L}}_j^{(n)}(t), \quad t \in \mathcal{T}_n, \quad n = 1, \ldots, N.$$

Here we have the nodal values $u_j^{(n)} \in \mathbb{R}^{n_\mathrm{u}}$. In order to keep notational clutter to a minimum, we restrict the presentation to the case of no explicit switches ($n_\mathrm{w} = 1$). The extension to the case with explicit and implicit switches is straight-forward. The controls $\boldsymbol{\alpha}_+,\ \boldsymbol{\alpha}_0,\ \boldsymbol{\alpha}_-$ are approximated by piecewise constant functions

$$\hat{\boldsymbol{\alpha}}(t) \triangleq \alpha^{(n)} = [\boldsymbol{\alpha}_+^{(n)}, \boldsymbol{\alpha}_0^{(n)}, \boldsymbol{\alpha}_-^{(n)}]^T, \quad t \in \mathcal{T}_n, \quad n = 1, \ldots, N.$$

To end up with an NLP we discretize the Mayer type objective as $\phi(x_{K_N}^{(N)})$ and the differential equations by means of finite element wise collocation

$$\begin{aligned} 0 \quad &= \dot{\mathbf{X}}(t_i^{(n)}) - \mathbf{f}(\mathbf{X}(t_i^{(n)}), \mathbf{U}(t_i^{(n)}), \hat{\boldsymbol{\alpha}}(t_i^{(n)})), \quad i = 1, \ldots, K_n, \quad n = 1, \ldots, N, \\ \Leftrightarrow \quad 0 &= \sum_{j=0}^{K_n} x_j^{(n)} \dot{\mathcal{L}}_j^{(n)}(t_i^{(n)}) - \mathbf{f}(x_i^{(n)}, \mathbf{U}(t_i^{(n)}), \alpha^{(n)}), \quad i = 1, \ldots, K_n, \quad n = 1, \ldots, N. \end{aligned}$$

To enforce continuity of the differential states we add the constraints

$$x_{K_n}^{(n)} = x_0^{(n+1)}, \quad n = 1, \ldots, N-1.$$

Alternatively one could simply identify the variables $x_{K_n}^{(n)}$ and $x_0^{(n+1)}$. But this would couple the variables over the finite element boundaries what is usually not desired. The discretization of the boundary constraints leads to the NLP constraints

$$0 \geq \mathbf{r}\left(x_0^{(1)}, x_{K_N}^{(N)}\right).$$

Path constraints are enforced to hold at collocation points and vanishing constraints are

enforced to hold at finite element grid points

$$
\begin{aligned}
&0 \geq \mathbf{c}(x_i^{(n)}, \mathbf{U}(t_i^{(n)})), && i = 1, \ldots, K_n, \quad n = 1, \ldots, N, \\
&0 \geq -\alpha_+^{(n)} \, (\boldsymbol{\sigma}(t_0^{(n)}, x_0^{(n)}) - \varepsilon), && n = 1, \ldots, N, && \text{(12a)} \\
&0 \geq +\alpha_-^{(n)} \, (\boldsymbol{\sigma}(t_0^{(n)}, x_0^{(n)}) + \varepsilon), && n = 1, \ldots, N, && \text{(12b)} \\
&0 \geq +\alpha_0^{(n)} \, (\boldsymbol{\sigma}(t_0^{(n)}, x_0^{(n)}) - \varepsilon), && n = 1, \ldots, N, && \text{(12c)} \\
&0 \geq -\alpha_0^{(n)} \, (\boldsymbol{\sigma}(t_0^{(n)}, x_0^{(n)}) + \varepsilon), && n = 1, \ldots, N. && \text{(12d)}
\end{aligned}
$$

The relaxed SOS1 constraint $\boldsymbol{\alpha}(t) \in \operatorname{conv}(\mathbb{S}^3)$ gets to the NLP constraints

$$
\sum_{j \in \{-,0,+\}} \alpha_j^{(n)} = 1, \quad \alpha_i^{(n)} \in [0, +\infty), \quad i \in \{-, 0, +\}, \quad n = 1, \ldots, N.
$$

4. Numerical Handling of Vanishing Constraints

The vanishing constraint structure of (11a–11d) is transferred to the discretized NLP constraints (12a–12d). More general, an NLP of the form

$$
\begin{aligned}
\min_{x \in \mathbb{R}^n} \quad & \psi(x) && && \text{(MPVC)} \\
\text{s.t.} \quad & 0 = \mathbf{s}_i(x), && i \in \mathcal{E}, \\
& 0 \geq \mathbf{s}_i(x), && i \in \mathcal{I}, \\
& 0 \geq \mathbf{h}(x), \\
& 0 \geq \mathbf{g}_i(x) \, \mathbf{h}_i(x), && i = 1, \ldots, m,
\end{aligned}
$$

where ψ, $\mathbf{s}$, $\mathbf{g}$ and $\mathbf{h}$ are $\mathcal{C}^2$ functions is called a Mathematical Program with Vanishing Constraints (MPVC), cf. [1]. It is easy to verify that the collocation NLP of the previous section is of MPVC type. MPVCs are highly non-convex optimization problems. All critical points violate the Linear Independence Constraint Qualification (LICQ). Even the weaker Mangasarian–Fromovitz Constraint Qualification (MFCQ) is violated, cf. [43]. Numerical solvers tend to terminate in suboptimal points with trivial descent directions. However, the Guignard Constraint Qualification (GCQ) holds, cf. [27]. For this reason, stationary points are still Karush–Kuhn–Tucker (KKT) points.

4.1 *Relaxation Formulation*

A common approach for solving MPVCs using standard nonlinear programming software originated in the field of mathematical programs with equilibrium constraints [54] and is in particular advocated for MPVCs [31, Chapter 10]. The approach pursues the idea of embedding (MPVC) into a family of perturbed problems parameterized by a scalar

perturbation $\tau > 0$. Problem (MPVC) may be embedded into the problem family

$$\begin{aligned} \min_{x\in\mathbb{R}^n} \quad & \phi(x) && && \text{(MPVC}(\tau)\text{)} \\ \text{s.t.} \quad & 0 = \mathbf{s}_i(x), && i \in \mathcal{E}, \\ & 0 \geq \mathbf{s}_i(x), && i \in \mathcal{I}, \\ & 0 \geq \mathbf{h}(x), \\ & \tau \geq \mathbf{g}_i(x)\,\mathbf{h}_i(x), && i = 1, \ldots, m, \end{aligned}$$

where $\tau > 0$ is the regularization parameter. The feasible set of (MPVC(τ)) relaxes the one of (MPVC). For $\tau \to 0^+$, the feasible set approaches the one of (MPVC). Other relaxation formulations are possible (see, e.g., [31]) but have not performed better than (MPVC(τ)) on the numerical examples provided below.

4.2 *Relaxation Homotopy, Backtracking, Adaptive Refinement*

In this section we describe in detail how we apply the method from the previous section to the MPVCs arising from the OCP discretization described in Section 3. Our numerical experiments have shown that it is important to couple the discretization accuracy with the homotopy parameter to avoid infeasible NLPs along the homotopy path.

We denote the value of the relaxation parameter in the k-th iteration by τ_k. Starting with an initial assignment for the relaxation parameter τ_0 we solve a sequence of NLPs. The relaxation parameter is driven to zero according to the rule

$$\tau_k = \gamma\,\tau_{k-1}, \quad k \geq 1, \quad \gamma \in (0, 1). \tag{13}$$

The NLP solver is initialized in iteration k with the NLP solution of iteration $k-1$. If the NLP in iteration k is infeasible we refine the finite element grid adaptively and solve the NLP again with the current relaxation parameter τ_k. In case the new NLP is feasible we continue applying rule (13). Otherwise the finite element grid is refined again. After a refinement step we initialize the NLP variables as follows: we take the NLP solver result from the previous iteration even if the NLP was infeasible. Compared to other strategies this was the one that worked the best in our experiments. Then we initialize all states and controls on the refined grid by interpolation.

Due to lack of a priori knowledge about the switching structure we usually start with an equidistant finite element grid. If NLP infeasiblities arise it is often because a switching point is not well resolved by the grid points. Hence our refinement algorithm has to take this into account.

We propose the following simple heuristic to refine the grid in order to resolve switching points: To this end, we construct a cubic spline interpolant $s(t)$ of each component of $\boldsymbol{\alpha}(t)$ in the element interface nodes $t_j, j = 0, \ldots, N$. We adaptively bisect a grid cell $[t_i, t_{i+1}]$ into two equally sized cells if either

$$\left| s'\left(\frac{t_{i-1}+t_i}{2}\right)\right| > \frac{1}{4}\max_{j=1,\ldots,N}\left\{\left|s'\left(\frac{t_{j-1}+t_j}{2}\right)\right|\right\} \tag{14}$$

$$\text{or} \quad |s''(t_i)| > \frac{1}{4}\max_{j=1,\ldots,N}\{|s''(t_j)|\}. \tag{15}$$

This heuristic detects high slopes of $\boldsymbol{\alpha}$ through (14), which indicates that a switch should

happen at some place within the interval, and high curvature of $\boldsymbol{\alpha}$ through (15), which indicates that a Filippov arc should begin or end at some place within the interval.

5. Numerical Results

In this section we demonstrate the applicability of our approach on three different benchmark problems. The first problem is a time optimal control problem and exhibits consistent switching behavior. Problem two and three are initial value problems with inconsistent switches.

5.1 *A Coulombic Friction Model*

We consider the model with consistent switches in [18] where a copper coil is guided in the air gap on a slider. The coil and slider mass is denoted by m_1. The Coulombic friction force F_R, which acts in the direction opposite to the velocity is produced by the linear guide. A load mass m_2 is mounted on the slider with a spring k that has negligible damping. A coil current I induces the actuating force $\mathbf{F}(t) = K_F\,\mathbf{I}(t)$. The moving coil with the velocity $\mathbf{v}_1$ generates a voltage $\mathbf{U}(t) = K_S\,\mathbf{v}_1(t)$.

The system states are the motor mass position $\mathbf{x}_1(t)$, the motor mass velocity $\mathbf{v}_1(t)$, the load mass position $\mathbf{x}_2(t)$, the load mass velocity $\mathbf{v}_2(t)$ and the electric current $\mathbf{I}(t)$. The control variable of the motor is the voltage $\mathbf{U}(t)$. The piecewise linear model equation reads as

$$\dot{\mathbf{x}}(t) = \mathbf{f}(\mathbf{x}(t), \mathbf{U}(t)),$$

where the state vector is denoted by $\mathbf{x}(t) = [\mathbf{x}_1(t), \mathbf{v}_1(t), \mathbf{x}_2(t), \mathbf{v}_2(t), \mathbf{I}(t)]^T$. The right hand side function $\mathbf{f}(\mathbf{x}(t), \mathbf{U}(t)) = [\mathbf{f}_1, \mathbf{f}_2, \mathbf{f}_3, \mathbf{f}_4, \mathbf{f}_5](\mathbf{x}(t), \mathbf{U}(t))^T$ is given as

$$\begin{aligned}
&\mathbf{f}_1(\mathbf{x}(t), \mathbf{U}(t)) = \mathbf{v}_1(t),\\
&\mathbf{f}_2(\mathbf{x}(t), \mathbf{U}(t)) = \left(K_F\,\mathbf{I}(t) - k\,(\mathbf{x}_1(t) - \mathbf{x}_2(t)) - F_R\,\operatorname{sgn}(\mathbf{v}_1(t))\right)/m_1,\\
&\mathbf{f}_3(\mathbf{x}(t), \mathbf{U}(t)) = \mathbf{v}_2(t),\\
&\mathbf{f}_4(\mathbf{x}(t), \mathbf{U}(t)) = k\,(\mathbf{x}_1(t) - \mathbf{x}_2(t))/m_2,\\
&\mathbf{f}_5(\mathbf{x}(t), \mathbf{U}(t)) = \left(\mathbf{U}(t) - R\,\mathbf{I}(t) - K_S\,\mathbf{v}_1(t)\right)/L.
\end{aligned}$$

The time horizon of the system is given by the interval $[0, t_f]$. We want to investigate the system on the unified time horizon $[0, 1]$. This can be achieved by the linear time transformation $t(\tau) = \tau\,t_f$, $\tau \in [0, 1]$. We choose t_f as an additional variable to achieve a system with free final time. Define

$$\bar{\mathbf{x}}(\tau) = \mathbf{x}(t(\tau)), \quad \bar{\mathbf{U}}(\tau) = \mathbf{U}(t(\tau)).$$

Then we obtain the equivalent transformed problem

$$\frac{d}{d\tau}\bar{\mathbf{x}}(\tau) = t_f\,\mathbf{f}(\bar{\mathbf{x}}(\tau), \bar{\mathbf{U}}(\tau)).$$

For the sake of clarity we use $\mathbf{x}(t)$ and $\mathbf{U}(t)$ instead of $\bar{\mathbf{x}}(\tau)$ and $\bar{\mathbf{U}}(\tau)$ in the remainder of

this section. The model parameters are given in Table 1. There are control box constraints

$$-U_{\max} \leq \mathbf{U}(t) \leq +U_{\max}$$

and initial as well as terminal state constraints

$$\mathbf{x}(0) = [0,0,0,0,0]^T, \qquad \mathbf{x}(1) = [0.01,0,0.01,0,0]^T.$$

We consider the minimal time cost functional

$$\min t_{\mathrm{f}},$$

and apply our approach to the resulting OCP. A switch is induced by the Coulombic friction force $-F_R\ \mathrm{sgn}(\mathbf{v}_1(t))$. The right hand side discontinuity is a consistent switch. Therefore we distinguish the two cases $-F_R$, if $\mathbf{v}_1(t) \geq 0$ and $+F_R$, if $\mathbf{v}_1(t) \leq 0$ for the Coulombic friction. We model this by introducing additional controls $\boldsymbol{\omega}(t) = [\boldsymbol{\omega}_{\geq}(t), \boldsymbol{\omega}_{\leq}(t)]^T$, $\boldsymbol{\omega}_{\geq}(t), \boldsymbol{\omega}_{\leq}(t) \in \{0,1\}$. Then the Coulombic friction force can be written as $-F_R\,(\boldsymbol{\omega}_{\geq}(t) - \boldsymbol{\omega}_{\leq}(t))$ if the two implications

$$\begin{aligned}
[\boldsymbol{\omega}_{\geq}(t) = 1 \implies \mathbf{v}_1(t) \geq 0] \quad &\iff \quad [-\mathbf{v}_1(t)\,\boldsymbol{\omega}_{\geq}(t) \leq 0],\\
[\boldsymbol{\omega}_{\leq}(t) = 1 \implies \mathbf{v}_1(t) \leq 0] \quad &\iff \quad [+\mathbf{v}_1(t)\,\boldsymbol{\omega}_{\leq}(t) \leq 0],
\end{aligned}$$

and the SOS1 constraint $\boldsymbol{\omega}_{\leq}(t) + \boldsymbol{\omega}_{\geq}(t) = 1$ hold. In the next step we replace the binary variables $\boldsymbol{\omega}_{\geq}(t), \boldsymbol{\omega}_{\leq}(t)$ by convexified control variables $\boldsymbol{\alpha}_{\geq}(t), \boldsymbol{\alpha}_{\leq}(t) \in [0,1]$. The resulting OCP now reads as

$$\begin{aligned}
\min_{t_f, \mathbf{x}(\cdot), \mathbf{U}(\cdot), \boldsymbol{\alpha}_{\geq}(\cdot), \boldsymbol{\alpha}_{\leq}(\cdot)} \quad & t_f \\
\text{s.t.} \quad & \dot{\mathbf{x}}_1(t) = t_f\,\mathbf{v}_1(t),\\
& \dot{\mathbf{v}}_1(t) = t_f\,\left(K_F\,\mathbf{I}(t) - k\,(\mathbf{x}_1(t) - \mathbf{x}_2(t)) - F_R\,(\boldsymbol{\alpha}_{\geq}(t) - \boldsymbol{\alpha}_{\leq}(t))\right)/m_1,\\
& \dot{\mathbf{x}}_2(t) = t_f\,\mathbf{v}_2(t),\\
& \dot{\mathbf{v}}_2(t) = t_f\,k\,(\mathbf{x}_1(t) - \mathbf{x}_2(t))/m_2,\\
& \dot{\mathbf{I}}(t) \;\; = t_f\,\left(\mathbf{U}(t) - R\,\mathbf{I}(t) - K_S\,\mathbf{v}_1(t)\right)/L,\\
& 0 \;\; \geq \; -\mathbf{v}_1(t)\,\boldsymbol{\alpha}_{\geq}(t),\\
& 0 \;\; \geq \; +\mathbf{v}_1(t)\,\boldsymbol{\alpha}_{\leq}(t),\\
& 1 \;\; = \boldsymbol{\alpha}_{\geq}(t) + \boldsymbol{\alpha}_{\leq}(t), \quad \boldsymbol{\alpha}_{\geq}(t), \boldsymbol{\alpha}_{\leq}(t) \in [0,1]. \qquad (16a)
\end{aligned}$$

Finally we eliminate $\boldsymbol{\alpha}_{\leq}(t)$: due to equation (16a) this can easily be done by replacing

Table 1. Parameters of the coulombic friction model

Physical quantity	Identifier	Value	Unit
Coil resistance	R	2	Ω
Coil inductivity	L	2	mH
Force constant	K_F	12	N/A
Voltage constant	K_S	12	Vs/m
Motor mass (slider, guide, coil)	m_1	1.03	kg
Load mass	m_2	0.56	kg
Spring constant	k	2.4	kN/m
Guide friction force	F_R	2.1	N

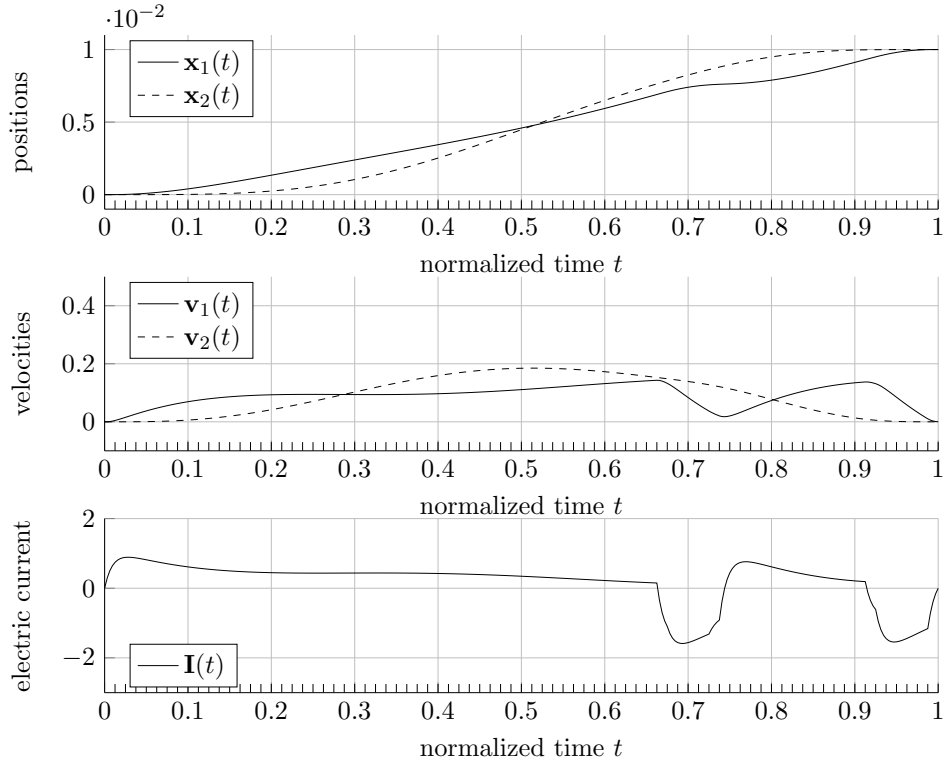

(a) Case: $U_{\max} = 2$.

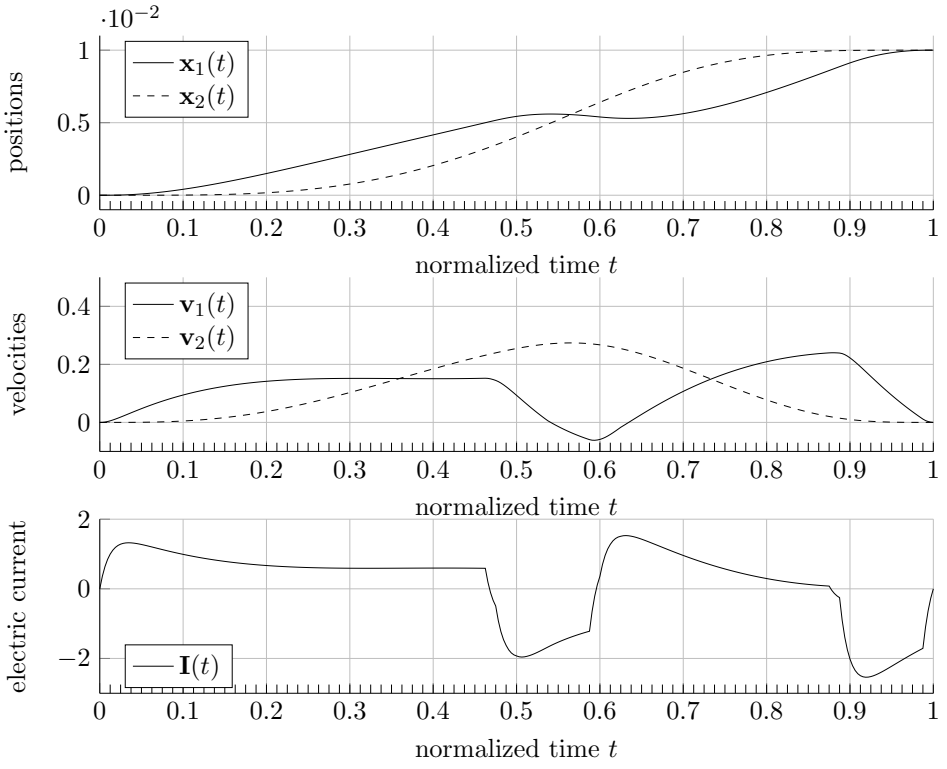

(b) Case: $U_{\max} = 3$.

Figure 1. State trajectories of the coulombic friction model from [18] with two different values for control bounds $U_{\max}$ and minimal time objective functional. Compared to [18] all trajectories show structurally the same behavior.

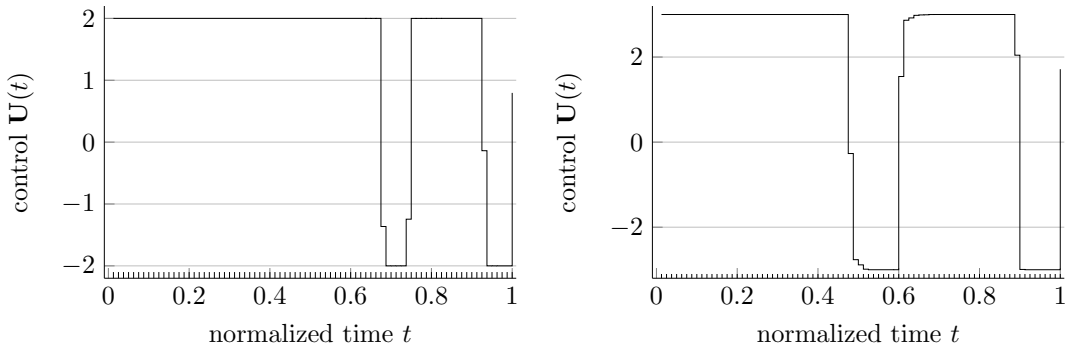

(a) Case: $U_{\max} = 2$. (b) Case: $U_{\max} = 3$.

Figure 2. Control profiles for two different values of $U_{\max}$ of the coulombic friction model from [18]. Compared to [18] we see the same structural behavior. Due to lack of refinement steps the bang-bang control in both plots is not fully pronounced.

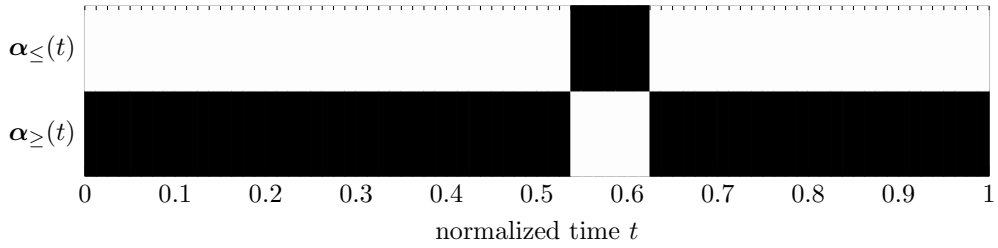

Figure 3. Mode switching profile for control bound choice $U_{\max} = 3$ of the coulombic friction model from [18]. One can see the chosen finite element grid indicated by ticks on the upper axis of the plot. The grayscale colors associated with each mode range from white (mode is not active) to black (mode is active). The plot shows that in the beginning and in the end mode $\boldsymbol{\alpha}_{\geq}$ is active. In between mode $\boldsymbol{\alpha}_{\leq}$ is active. This result coincides with the plot in Figure 1(b) where the sign of $\mathbf{v}_1$ matches with chosen modes in this plot.

$\boldsymbol{\alpha}_{\leq}(t)$ with $1 - \boldsymbol{\alpha}_{\geq}(t)$ in all equations of problem (16). Equation (16a) then reduces to $\boldsymbol{\alpha}_{\geq}(t) \in [0, 1]$.

Then we discretize the OCP as described in Section 3 with 80 equidistant finite elements, polynomial order 2 for states and polynomial order 0 for control $\mathbf{U}$. The technique described in Section 4.1 is applied to solve the resulting MPVC. We choose $\tau_0 = 10^{-3}$ as the initial regularization parameter. The regularization parameter is reduced in each iteration according to the rule $\tau_k = \sqrt{0.9}\,\tau_{k-1}$, $k \geq 1$. The arising NLPs are solved with the sparse sequential quadratic programming (SQP) solver SNOPT [23] without adaptive mesh refinement. We apply the default settings of SNOPT.

Figure 5.1 shows the resulting state trajectories for chosen control bounds $U_{\max} = 2$ and $U_{\max} = 3$ returned by SNOPT. One can see that the state trajectories show structurally the same behavior compared to the results in [18]. We cannot compare the results in detail because the value for parameter K_S is missing in [18]. In Figure 2 the control trajectory of $\mathbf{U}$ is depicted for both control bound choices. Figure 3 provides for control bound $U_{\max} = 3$ a view of the chosen modes represented by the control trajectories of $\boldsymbol{\alpha}_{\leq}$ and $\boldsymbol{\alpha}_{\geq}$. For case $U_{\max} = 2$ we are permanently in mode $\boldsymbol{\alpha}_{\geq} = 1$ and $\boldsymbol{\alpha}_{\geq} = 0$. Therefore we do not show the corresponding plot.

5.2 *A Stick-Slip Model with Known Switching Point*

We consider the following inconsistently switched model

$$\dot{\mathbf{x}}(t) = \begin{bmatrix} \mathbf{x}_2(t) \\ -\frac{k}{m}\mathbf{x}_1(t) + \frac{\mathbf{F}(\mathbf{x}_1(t),\mathbf{v}_{\text{rel}}(t))}{m} \end{bmatrix}, \tag{17}$$

where $\mathbf{x}(t) = [\mathbf{x}_1(t), \mathbf{x}_2(t)]^T$ and $\mathbf{v}_{\text{rel}}(t) = \mathbf{x}_2(t) - v_b$. The friction force $\mathbf{F}$ is a function of the relative velocity $\mathbf{v}_{\text{rel}}$ in the slip phase and a function of the spring force kx in the stick phase:

$$\mathbf{F}(x, v_{\text{rel}}) = \begin{cases} \min(|kx|, F_s)\ \text{sgn}(kx), & v_{\text{rel}} = 0 \qquad \text{stick}, \\ -F_s\, v_{\text{rel}}, & v_{\text{rel}} \neq 0 \qquad \text{slip} \end{cases} \tag{18}$$

A simple calculation shows that starting from the initial value $\mathbf{x}(0) = [0, 1]^T$, the first switch from the sticking mode to the slipping mode occurs at time $t = F_s/k$.

We apply our approach to the initial value problem: first we replace the stick mode triggering constraint $\mathbf{v}_{\text{rel}}(t) = 0$ by a relaxed constraint $-\varepsilon \leq \mathbf{v}_{\text{rel}}(t) \leq \varepsilon$. The stick-slip branches, the $\text{sgn}(\cdot)$, $\min(\cdot,\cdot)$ and the $|\cdot|$ functions in (18) induce state dependent switches. One identifies five modes in the model if all switches are taken into account. Therefore we introduce controls $\boldsymbol{\alpha}(t) = [\boldsymbol{\alpha}_1(t), \ldots, \boldsymbol{\alpha}_5(t)]^T$, $\boldsymbol{\alpha}_i(t) \in [0, 1],\ i = 1, \ldots, 5$. The five modes are characterized by the following implications:

$$\boldsymbol{\alpha}_1(t) = 1 \implies -\varepsilon \leq \mathbf{v}_{\text{rel}}(t) \leq +\varepsilon \ \wedge\ |k\mathbf{x}_1(t)| \leq F_s \tag{19}$$

$$\boldsymbol{\alpha}_2(t) = 1 \implies -\varepsilon \leq \mathbf{v}_{\text{rel}}(t) \leq +\varepsilon \ \wedge\ k\mathbf{x}_1(t) \leq -F_s \tag{20}$$

$$\boldsymbol{\alpha}_3(t) = 1 \implies -\varepsilon \leq \mathbf{v}_{\text{rel}}(t) \leq +\varepsilon \ \wedge\ k\mathbf{x}_1(t) \geq +F_s \tag{21}$$

$$\boldsymbol{\alpha}_4(t) = 1 \implies \mathbf{v}_{\text{rel}}(t) \geq +\varepsilon \tag{22}$$

$$\boldsymbol{\alpha}_5(t) = 1 \implies \mathbf{v}_{\text{rel}}(t) \leq -\varepsilon \tag{23}$$

The reformulated model equations (17)-(18), the vanishing constraint formulations of implications (19)-(23) and the convexified SOS1 constraint $\boldsymbol{\alpha}(t) \in \text{conv}(\mathbb{S}^5)$ yield the

Table 2. Parameters of the stick-slip model

Physical quantity	Identifier	Value	Unit
Spring constant	k	1.0	Nm
Mass	m	1.0	kg
Relative belt vel.	v_b	1.0	m/s
Max. stat. friction force	F_s	0.45,0.5	N
Relaxation parameter	ε	10^{-15}	-

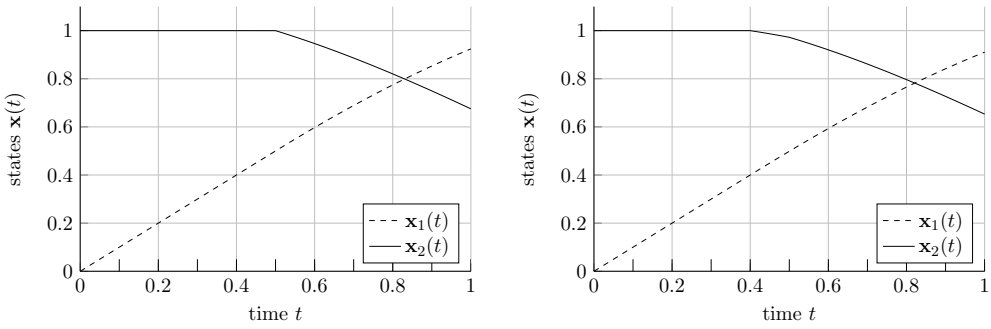

(a) Case: $F_s = 0.5$. The exact switching point at time $t = 0.5$ is part of the finite element grid. Our approach detects the switch exactly, as indicated by the kink of the $\mathbf{x}_2$ trajectory.

(b) Case: $F_s = 0.45$. The exact switching point at time $t = 0.45$ is not part of the finite element grid. Our approach detects the switch too early indicated by the kink of the $\mathbf{x}_2$ trajectory at time $t = 0.4$.

Figure 4. State trajectories of the stick-slip model for two different assignments for parameter F_s. In both cases we choose 10 equidistant finite elements.

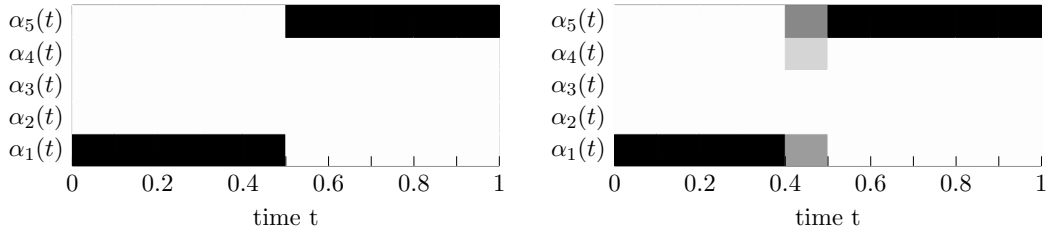

(a) Case: $F_s = 0.5$. The analytical switching point from mode 1 ($\boldsymbol{\alpha}_1(t) = 1$) to mode 5 ($\boldsymbol{\alpha}_1(t) = 1$) is at time $t = 0.5$. This can also be seen in the plot.

(b) Case: $F_s = 0.45$. The analytical switching point from mode 1 ($\boldsymbol{\alpha}_1(t) = 1$) to mode 5 ($\boldsymbol{\alpha}_1(t) = 1$) is at time $t = 0.45$. The plot shows that in the finite element interval [0.4,0.5] where the switch takes place, there are three partially active modes.

Figure 5. Element-wise partitions indicating the active modes of the stick-slip model for two different assignments of parameter F_s. In both cases we choose 10 equidistant finite elements indicated by ticks in both plots. The grayscale colors associated with each mode range from white (mode is not active) to black (mode is active).

following feasibility problem:

$$
\begin{aligned}
\text{find} \quad & \mathbf{x}(\cdot),\ \boldsymbol{\alpha}(\cdot) \\
\text{s.t.} \quad & \dot{\mathbf{x}}_1(t) \;=\; \mathbf{x}_2(t), \\
& \dot{\mathbf{x}}_2(t) \;=\; \big((\boldsymbol{\alpha}_1(t) - 1)\, k\, \mathbf{x}_1(t) + F_s\, \mathbf{v}_{\mathrm{rel}}(t)\ (\boldsymbol{\alpha}_3(t) - \boldsymbol{\alpha}_2(t))\big)/m \\
(19) \Leftrightarrow \quad & \mathbf{0} \;\geq\; [-\varepsilon + \mathbf{v}_{\mathrm{rel}}(t), -\varepsilon - \mathbf{v}_{\mathrm{rel}}(t), -F_s + k\, \mathbf{x}_1(t), -F_s - k\, \mathbf{x}_1(t)]^T\, \boldsymbol{\alpha}_1(t) \\
(20) \Leftrightarrow \quad & \mathbf{0} \;\geq\; [-\varepsilon + \mathbf{v}_{\mathrm{rel}}(t), -\varepsilon - \mathbf{v}_{\mathrm{rel}}(t), +F_s + k\, \mathbf{x}_1(t)]^T\, \boldsymbol{\alpha}_2(t) \\
(21) \Leftrightarrow \quad & \mathbf{0} \;\geq\; [-\varepsilon + \mathbf{v}_{\mathrm{rel}}(t), -\varepsilon - \mathbf{v}_{\mathrm{rel}}(t), +F_s - k\, \mathbf{x}_1(t)]^T\, \boldsymbol{\alpha}_3(t) \\
(22) \Leftrightarrow \quad & 0 \;\geq\; [+\varepsilon - \mathbf{v}_{\mathrm{rel}}(t)]\, \boldsymbol{\alpha}_4(t) \\
(23) \Leftrightarrow \quad & 0 \;\geq\; [+\varepsilon + \mathbf{v}_{\mathrm{rel}}(t)]\, \boldsymbol{\alpha}_5(t) \\
& 1 \;=\; \sum\nolimits_{j=1}^{5} \boldsymbol{\alpha}_j(t), \quad \boldsymbol{\alpha}_i(t) \in [0,1], \quad i = 1, \ldots, 5.
\end{aligned}
$$

The feasibility problem is discretized with the techniques from Section 3. We choose an equidistant grid with 10 finite elements and a polynomial order 2 for the state approxi-

mation polynomials. Model parameters and ε assignment are given in Table 2. One can see that we choose two different values for parameter F_s. For $F_s = 0.5$ the switching point of the system is a finite element grid point whereas for $F_s = 0.45$ the switching point is in the middle of the finite element interval $[0.4, 0.5]$. The two discretized systems are then solved with SNOPT. In both cases default options for SNOPT are chosen. SNOPT can solve the system without the regularization approach to handle the vanishing constraints.

Figure 4 shows the resulting state trajectories for $F_s = 0.45$ and $F_s = 0.5$. Analogously Figure 5 depicts the chosen modes for both cases.

As can be seen in Figure 4(b), in the case $F_s = 0.45$ our approach detects a switch from the stick to the slip mode at time $t = 0.4$ indicated by the kink of the $\mathbf{x}_2$ trajectory at time $t = 0.4$. According to the analytical solution the switch actually occurs at time $t = F_s/k = 0.45$. In this case we cannot expect the switching time to be detected at the analytically correct time, because the time $t = 0.45$ is not part of the finite element grid. Figure 5(b) illustrates this: apart from the switch point including finite element interval [0.4,0.5] there is either mode 1 ($\boldsymbol{\alpha}_1(t) = 1$) oder mode 5 ($\boldsymbol{\alpha}_5(t) = 1$) active. In [0.4,0.5] fractions of mode 1, 4 and 5 are active.

In the case of $F_s = 0.5$ our approach detects the first switch at time $t = 0.5$. This can either be seen in Figure 4(a) indicated by the kink of the $\mathbf{x}_2$ trajectory at time $t = 0.5$ or by the mode switching event from finite element interval [0.4,0.5] to [0.5,0.6] illustrated in Figure 5(a). The formula $t = F_s/k = 0.5$ confirms the switching point for the analytical solution. The accordance of predicted and analytical switching time could be explained by the fact that the switching time is part of the finite element grid.

This example makes clear that it is indispensable for our approach to develop reliable refinement strategies. Only if one can detect switching points up to a certain level of accuracy reliable solutions can be expected. But our experiments also give rise to hopes that the values of the mode controls $\boldsymbol{\alpha}$ give good indications in which finite element intervals the switches are located.

5.3 *An Alternate Friction Model*

We consider the inconsistently switched model in [40] and [41] where a mass m is attached to an inertial space by a spring with spring constant k. The mass is sliding on a driving belt. The belt is moving at constant velocity v_b. Dry friction with a friction force F occurs between mass and belt. The model equations read as

$$\dot{\mathbf{x}}(t) = \begin{bmatrix} \mathbf{x}_2(t) \\ -\frac{k}{m}\mathbf{x}_1(t) + \frac{\mathbf{F}(\mathbf{x}_1(t), \mathbf{v}_{\text{rel}}(t))}{m} \end{bmatrix}, \tag{24}$$

where $\mathbf{x}(t) = [\mathbf{x}_1(t), \mathbf{x}_2(t)]^T$ and $\mathbf{v}_{\text{rel}}(t) = \mathbf{x}_2(t) - v_b$. The friction force $\mathbf{F}$ is a function of the relative velocity $\mathbf{v}_{\text{rel}}$ in the slip phase and a function of the spring force kx in the stick phase

$$\mathbf{F}(x, v_{\text{rel}}) = \begin{cases} \min(|kx|, F_s)\ \operatorname{sgn}(kx), & v_{\text{rel}} = 0 \quad \text{stick}, \\ -\frac{F_s \operatorname{sgn}(v_{\text{rel}})}{1+\delta\,|v_{\text{rel}}|}, & v_{\text{rel}} \neq 0 \quad \text{slip}. \end{cases} \tag{25}$$

The model parameters are depicted in Table 3. We solve the initial value problem with initial values $\mathbf{x}(t_0) = [1.133944669704, 0]^T$ on the horizon $\mathcal{T} = [0, 12]$.

State dependent switches are induced by the stick-slip branches, $\operatorname{sgn}(\cdot)$, $\min(\cdot,\cdot)$ and $|\cdot|$ functions in (25). In the following, we apply our approach: to this end we replace the

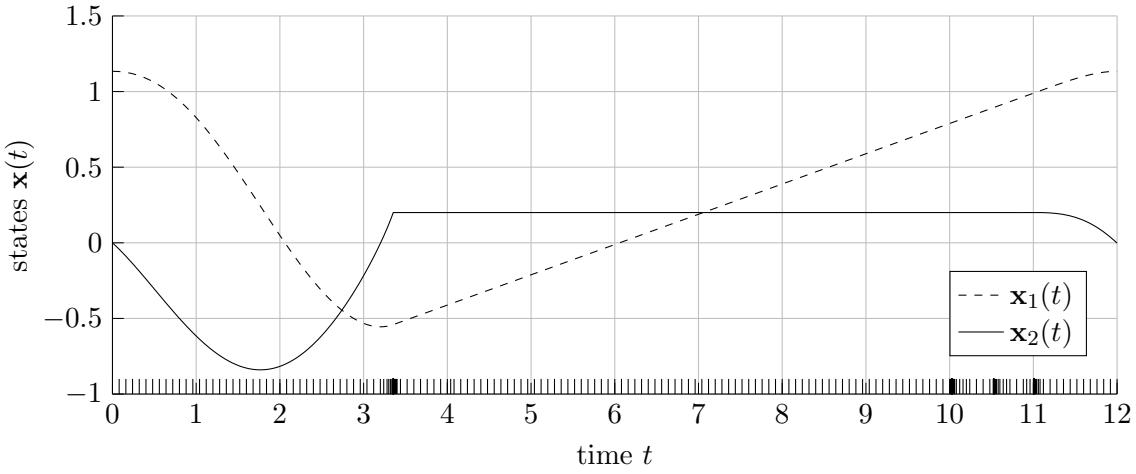

Figure 6. State trajectories of the switched alternate friction model ([40], [41]). The black tick marks on the lower axis indicate the element boundaries, which accumulate at the switch points to accurately resolve the switching times.

stick mode triggering constraint $\mathbf{v}_{\text{rel}}(t) = 0$ by a relaxed constraint $-\varepsilon \leq \mathbf{v}_{\text{rel}}(t) \leq \varepsilon$. We then identify five modes in the model and introduce controls $\boldsymbol{\alpha}(t) = [\boldsymbol{\alpha}_1(t), \ldots, \boldsymbol{\alpha}_5(t)]^T$, $\boldsymbol{\alpha}_i(t) \in [0, 1]$. The five modes are characterized by the implications

$$\boldsymbol{\alpha}_1(t) = 1 \quad \Longrightarrow \quad -\varepsilon \leq \mathbf{v}_{\text{rel}}(t) \leq +\varepsilon \quad \wedge \quad |k\mathbf{x}_1(t)| \leq F_s, \tag{26}$$

$$\boldsymbol{\alpha}_2(t) = 1 \quad \Longrightarrow \quad -\varepsilon \leq \mathbf{v}_{\text{rel}}(t) \leq +\varepsilon \quad \wedge \quad k\mathbf{x}_1(t) \leq -F_s, \tag{27}$$

$$\boldsymbol{\alpha}_3(t) = 1 \quad \Longrightarrow \quad -\varepsilon \leq \mathbf{v}_{\text{rel}}(t) \leq +\varepsilon \quad \wedge \quad k\mathbf{x}_1(t) \geq +F_s, \tag{28}$$

$$\boldsymbol{\alpha}_4(t) = 1 \quad \Longrightarrow \quad \mathbf{v}_{\text{rel}}(t) \geq +\varepsilon, \tag{29}$$

$$\boldsymbol{\alpha}_5(t) = 1 \quad \Longrightarrow \quad \mathbf{v}_{\text{rel}}(t) \leq -\varepsilon. \tag{30}$$

The new formulated model equations (24)-(25), the mode characterizing implications (26)-(30) and the convexified SOS1 constraint $\boldsymbol{\alpha}(t) \in \text{conv}(\mathbb{S}^5)$ result in the following

Table 3. Parameters of the alternate friction model

Physical quantity	Identifier	Value	Unit
Spring constant	k	1.0	Nm
Mass	m	1.0	kg
Relative belt vel.	v_b	0.2	m/s
Max. stat. friction force	F_s	1.0	N
Phys. constant	δ	3.0	s/m
Relaxation parameter	ε	10^{-15}	-

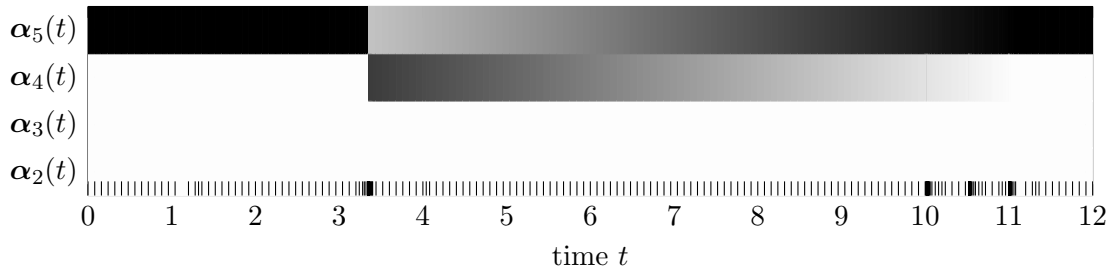

Figure 7. Element-wise partitions indicating the active modes in the alternate friction model ([40], [41]). The grayscale colors associated with each mode range from white (mode is not active) to black (mode is active). The plot shows that in the beginning and in the end mode 5 is active. In between there is a Filippov solution realized by convex combinations of modes 4 and 5. The black tick marks on the lower axis indicate the element boundaries, which accumulate at the switch points to accurately resolve the switching times.

feasibility problem:

$$
\begin{aligned}
&\text{find} && \mathbf{x}(\cdot),\ \boldsymbol{\alpha}(\cdot) \\
&\text{s.t.} && \dot{\mathbf{x}}_1(t) = \mathbf{x}_2(t), \\
& && \dot{\mathbf{x}}_2(t) = \mathbf{f}_2(\mathbf{x}(t), \boldsymbol{\alpha}(t)) \\
&(26) \Leftrightarrow && \mathbf{0} \geq [-\varepsilon + \mathbf{v}_{\text{rel}}(t), -\varepsilon - \mathbf{v}_{\text{rel}}(t), -F_s + k\,\mathbf{x}_1(t), -F_s - k\,\mathbf{x}_1(t)]^T\, \boldsymbol{\alpha}_1(t) \\
&(27) \Leftrightarrow && \mathbf{0} \geq [-\varepsilon + \mathbf{v}_{\text{rel}}(t), -\varepsilon - \mathbf{v}_{\text{rel}}(t), +F_s + k\,\mathbf{x}_1(t)]^T\, \boldsymbol{\alpha}_2(t) \\
&(28) \Leftrightarrow && \mathbf{0} \geq [-\varepsilon + \mathbf{v}_{\text{rel}}(t), -\varepsilon - \mathbf{v}_{\text{rel}}(t), +F_s - k\,\mathbf{x}_1(t)]^T\, \boldsymbol{\alpha}_3(t) \\
&(29) \Leftrightarrow && 0 \geq [+\varepsilon - \mathbf{v}_{\text{rel}}(t)]\, \boldsymbol{\alpha}_4(t) \\
&(30) \Leftrightarrow && 0 \geq [+\varepsilon + \mathbf{v}_{\text{rel}}(t)]\, \boldsymbol{\alpha}_5(t) \\
& && 1 = \sum\nolimits_{j=1}^{5} \boldsymbol{\alpha}_j(t), \quad \boldsymbol{\alpha}_i(t) \in [0,1], \quad i = 1, \ldots, 5,
\end{aligned}
\tag{31a}
$$

where

$$
\mathbf{f}_2(\mathbf{x}(t), \boldsymbol{\alpha}(t)) = \frac{(\boldsymbol{\alpha}_1(t) - 1)\, k\, \mathbf{x}_1(t) + F_s \left(\boldsymbol{\alpha}_3(t) - \boldsymbol{\alpha}_2(t) + \frac{\boldsymbol{\alpha}_5(t)}{1 - \delta\, \mathbf{v}_{\text{rel}}(t)} - \frac{\boldsymbol{\alpha}_4(t)}{1 + \delta\, \mathbf{v}_{\text{rel}}(t)} \right)}{m}. \tag{32}
$$

We apply the discretization strategy described in Section 3, where we choose an equidistant finite element grid with 150 elements and polynomial order 3 to approximate the states. Before solving the arising MPVCs, we investigate the problem further for the case $\varepsilon = 0$: Based on physical insight, we expect that there is an interval with $\mathbf{v}_{\text{rel}}(t) = 0$. If we set $\mathbf{v}_{\text{rel}}(t) = 0$ in (32) and assume that mode 1 is active ($\boldsymbol{\alpha}_1(t) = 1,\ \boldsymbol{\alpha}_2(t), \ldots, \boldsymbol{\alpha}_5(t) = 0$) then $\mathbf{f}_2(\mathbf{x}(t), \boldsymbol{\alpha}(t))$ is equal to zero. On the other hand if we set $\mathbf{v}_{\text{rel}}(t) = 0$ and assume $|k\mathbf{x}_1(t)| \leq F_s$, we can use (31a) to eliminate the explicit appearance of $\boldsymbol{\alpha}_1$ to obtain

$$
\begin{aligned}
0 =& \frac{-k\,\mathbf{x}_1(t)\,(\boldsymbol{\alpha}_3(t) + \boldsymbol{\alpha}_2(t) + \boldsymbol{\alpha}_5(t) + \boldsymbol{\alpha}_4(t)) + F_s\,(\boldsymbol{\alpha}_3(t) - \boldsymbol{\alpha}_2(t) + \boldsymbol{\alpha}_5(t) - \boldsymbol{\alpha}_4(t))}{m} \\
=& \frac{+F_s - k\,\mathbf{x}_1(t)}{m}(\boldsymbol{\alpha}_3(t) + \boldsymbol{\alpha}_5(t)) + \frac{-F_s - k\,\mathbf{x}_1(t)}{m}(\boldsymbol{\alpha}_2(t) + \boldsymbol{\alpha}_4(t)),
\end{aligned}
\tag{33}
$$

which is a linear combination of the right hand side terms corresponding to modes 4 and 5. This observation yields the link to Filippov solutions of the switched system (24)–(25).

To this end, we reformulate the system in the sense of Filippov by only describing the dynamics of the the two slip modes ($v_{\text{rel}} > 0$ and $v_{\text{rel}} < 0$). This can be achieved by replacing $\mathbf{F}$ with

$$\hat{\mathbf{F}}(x, v_{\text{rel}}) = \begin{cases} -\frac{F_s}{1+\delta v_{\text{rel}}}, & v_{\text{rel}} \geq 0, \\ +\frac{F_s}{1-\delta v_{\text{rel}}}, & v_{\text{rel}} \leq 0, \end{cases}$$

which is multi-valued in $v_{\text{rel}} = 0$. We then construct Filippov solutions for the stick phase ($v_{\text{rel}} = 0$) by a convex combination of the right hand side traces $-F_s$ and $+F_s$ on the switch manifold $v_{\text{rel}} = 0$. Apparently, the Filippov approach coincides with our approach only if the linear combination coefficients $\boldsymbol{\alpha}_3 + \boldsymbol{\alpha}_5$ and $\boldsymbol{\alpha}_2 + \boldsymbol{\alpha}_4$ in (33) add up to one. This implies $\boldsymbol{\alpha}_1 \equiv 0$. In fact, we can explicitly enforce Filippov solutions by bounding $\boldsymbol{\alpha}_1 \leq \tau \to 0$ within the homotopy approach to obtain satisfactory numerical solutions.

After discretization we apply the MPVC relaxation algorithm from Section 4.1 and the techniques described in Section 4.2 to the resulting finite dimensional feasibility problem with vanishing constraints. We choose $\tau_0 = 10^{-3}$ as initial regularization parameter and update it according to the rule $\tau_k = \sqrt{0.9}\,\tau_{k-1}$, $k \geq 1$. The arising NLPs are solved with the SQP solver SNOPT.

Figure 6 depicts the state trajectories resulting from our calculations. As can be seen in Figure 7 our approach detects a switch from the slipping mode to the sticking mode and back. The refinement scheme is important to accurately determine the switching points.

6. Conclusions

In this article, we have presented a novel approach to solving OCPs constrained by ordinary differential equations with explicitly as well as implicitly defined, state-dependent discontinuities in a unified framework. Our approach is based on binary indicator functions, an idea from generalized disjunctive programming, and on a direct and simultaneous adaptive collocation approach to optimal control, and results in mathematical programs with vanishing constraints. We applied our approach to three benchmark examples of hybrid systems. The proposed approach promises to be able to detect optimal switching structures, and to identify a non-classical solution in the case of inconsistent switching. Our computational results also show that optimal switching points in time can only be identified up to the time discretization grid granularity and therefore require adaptive grid refinement near switching points.

The numerical examples indicate extensions and highlight challenges for the reliable solution of inconsistently switched systems within our approach as well. The following questions need to be addressed in future research: Is it always better to not model the dynamics on the switch manifold in expectance of Filippov-type solutions for the multipliers $\boldsymbol{\alpha}$? Are continuous discretizations for $\boldsymbol{\alpha}$ advantageous on Filippov-type arcs in contrast to discontinuous piecewise constant discretizations used here (which are required at switch points)? How can adaptivity with respect to the arcs of continuous dynamics and with respect to the switching points be unified theoretically and numerically and orchestrated within the homotopy for the treatment of the vanishing constraint homotopy?

Funding

C. Kirches was supported by DFG Graduate School 220 (Heidelberg Graduate School of Mathematical and Computational Methods for the Sciences) funded by the German Excellence Initiative, and acknowledges financial support by the European Union within the 7$^{\text{th}}$ Framework Programme under Grant Agreement n$^{\text{o}}$ 611909 and by Deutsche Forschungsgemeinschaft through Priority Programme 1962 "Non-smooth and Complementarity-based Distributed Parameter Systems: Simulation and Hierarchical Optimization". C. Kirches, A. Meyer and A. Potschka acknowledge funding by the German Federal Ministry of Education and Research (BMBF) program "Mathematics for Innovations in Industry and Service", grants n$^{\text{o}}$ 05M2013-GOSSIP and n$^{\text{o}}$ 05M2016-MoPhaPro. A. Meyer and A. Potschka acknowledge funding by the European Research Council Adv. Inv. Grant MOBOCON 291 458.

References

[1] W. Achtziger and C. Kanzow, *Mathematical programs with vanishing constraints: optimality conditions and constraint qualifications*, Mathematical Programming Series A **114** (2008), 69–99.

[2] R.J. Allgor and P.I. Barton, *Mixed-integer dynamic optimization. I - Problem formulation*, Computers & Chemical Engineering **23** (1999), no. 4, 567–584.

[3] P. Antsaklis and X. Koutsoukos, *On hybrid control of complex systems: A survey*, In 3rd International Conference ADMP'98, Automation of Mixed Processes: Dynamic Hybrid Systems, March 1998, pp. 1–8.

[4] E. Balas, *Disjunctive Programming and a Hierarchy of Relaxations for Discrete Optimization Problems*, SIAM Journal on Algebraic and Discrete Methods **6** (1985), no. 3, 466–486.

[5] V. Bansal, V. Sakizlis, R. Ross, J.D. Perkins, and E.N. Pistikopoulos, *New algorithms for mixed-integer dynamic optimization*, Computers & Chemical Engineering **27** (2003), 647–668.

[6] B.T. Baumrucker and L.T. Biegler, *MPEC strategies for optimization of a class of hybrid dynamic systems*, Journal of Process Control **19** (2009), no. 8, 1248–1256, Special Section on Hybrid Systems: Modeling, Simulation and Optimization.

[7] A. Bemporad, F. Borrelli, and M. Morari, *Piecewise linear optimal controllers for hybrid systems*, Proceedings of the 2000 American Control Conference. ACC (IEEE Cat. No.00CH36334) **2** (2000), 1190–1194.

[8] A. Bemporad and M. Morari, *Control of systems integrating logic, dynamics, and constraints*, Automatica **35** (1999), no. 3, 407–427.

[9] A. Bemporad, G. Ferrari Trecate, and M. Morari, *Observability and controllability of piecewise affine and hybrid systems*, IEEE Transactions on Automatic Control **45** (1999), 1864–1876.

[10] S.C. Bengea and R.A. Decarlo, *Optimal control of switching systems*, Automatica **41** (2005), no. 1, 11–27.

[11] L.T. Biegler, *Solution of dynamic optimization problems by successive quadratic programming and orthogonal collocation*, Computers & Chemical Engineering **8** (1984), 243–248.

[12] H.G. Bock, *Randwertproblemmethoden zur Parameteridentifizierung in Systemen nichtlinearer Differentialgleichungen*, Bonner Mathematische Schriften, vol. 183, Universität Bonn, Bonn, 1987.

[13] H.G. Bock and K.J. Plitt, *A Multiple Shooting algorithm for direct solution of optimal control problems*, Proceedings of the 9th IFAC World Congress (Budapest), Pergamon Press, 1984, pp. 242–247.

[14] F. Borrelli, M. Baotic, A. Bemporad, and M. Morari, *An efficient algorithm for computing the state feedback optimal control law for discrete time hybrid systems*, Proceedings of the 2003 American Control Conference, 2003. **6** (2003), 4717–4722.

[15] ———, *Dynamic programming for constrained optimal control of discrete-time linear hybrid systems*, 2005, pp. 1709–1721.

[16] U. Brandt-Pollmann, *Numerical solution of optimal control problems with implicitly defined discontinuities with applications in engineering*, Ph.D. thesis, Universität Heidelberg, 2004.

[17] M.S. Branicky, V.S. Borkar, and S.K. Mitter, *A Unified Framework for Hybrid Control: Model and Optimal Control*, IEEE Transactions on Automatic Control **43** (1998), no. 1, 31–45.

[18] B. Christiansen, H. Maurer, and O. Zirn, *Optimal control of a voice-coil-motor with coulombic friction*, Proceedings of the IEEE Conference on Decision and Control, 2008, pp. 1557–1562.

[19] S. Engell, G. Frehse, and E. Schnieder, *Modelling, analysis and design of hybrid systems*, vol. 279, Springer, 2003.
[20] A.F. Filippov, *Differential Equations with discontinuous right hand side*, AMS Transl. **42** (1964), 199–231.
[21] D. Garg, M. A. Patterson, W. W. Hager, A. V. Rao, D. A. Benson, and G. T. Huntington, *An Overview of Three Pseudospectral Methods for the Numerical Solution of Optimal Control Problems*, Advances in the Astronautical Sciences **135** (2009), no. 1, 475–487.
[22] M. Gerdts and S. Sager, *Mixed-Integer DAE Optimal Control Problems: Necessary conditions and bounds*, Control and Optimization with Differential-Algebraic Constraints (L. Biegler, S.L. Campbell, and V. Mehrmann, eds.), SIAM, 2012, pp. 189–212.
[23] P.E. Gill, W. Murray, and M.A. Saunders, *SNOPT: An SQP algorithm for large-scale constrained optimization*, SIAM Journal of Optimization **12** (2002), 979–1006.
[24] R. Goebel, R. Sanfelice, and A.R. Teel, *Hybrid dynamical systems*, IEEE Control Systems Magazine **29** (2009), no. 2, 28–93.
[25] H. Gonzalez, R. Vasudevan, M. Kamgarpour, S.S. Sastry, R. Bajcsy, and C.J. Tomlin, *A Descent Algorithm for the Optimal Control of Constrained Nonlinear Switched Dynamical Systems*, Proceedings of the 13th International Conference on Hybrid Systems: Computation and Control, 2010, pp. 51–60.
[26] ———, *A Numerical Method for the Optimal Control of Switched Systems*, Proceedings of the 49th IEEE Conference on Decision and Control, 2010, pp. 7519–7526.
[27] M. Guignard, *Generalized Kuhn–Tucker conditions for mathematical programming problems in a Banach space*, SIAM Journal on Control **7** (1969), no. 2, 232–241.
[28] F.M. Hante and S. Sager, *Relaxation Methods for Mixed-Integer Optimal Control of Partial Differential Equations*, Computational Optimization and Applications **55** (2013), no. 1, 197–225.
[29] S. Hedlund and A. Rantzer, *Convex Dynamic Programming for Hybrid Systems*, IEEE Transactions on Automatic Control **47** (2002), no. 9, 1536–1540.
[30] I.A. Hiskens and M.A. Pai, *Trajectory sensitivity analysis of hybrid systems*, IEEE Transactions on Circuits and Systems I: Fundamental Theory and Applications **47** (2000), no. 2, 204–220.
[31] T. Hoheisel, *Mathematical Programs with Vanishing Constraints*, Ph.D. thesis, Julius–Maximilians–Universität Würzburg, July 2009.
[32] G. T. Huntington, D. Benson, A. V. Rao, et al., *A comparison of accuracy and computational efficiency of three pseudospectral methods*, Proceedings of the AIAA Guidance, Navigation, and Control Conference, 2007, pp. 840–864.
[33] J.I. Imura and A. Van Der Schaft, *Characterization of well-posedness of piecewise-linear systems*, IEEE Transactions on Automatic Control **45** (2000), no. 9, 1600–1619.
[34] M. Jung, C. Kirches, and S. Sager, *On Perspective Functions and Vanishing Constraints in Mixed-Integer Nonlinear Optimal Control*, Facets of Combinatorial Optimization – Festschrift for Martin Grötschel (M. Jünger and G. Reinelt, eds.), Springer Berlin Heidelberg, 2013, pp. 387–417.
[35] E.C. Kerrigan and D.Q. Mayne, *Optimal control of constrained, piecewise affine systems with bounded disturbances*, Proc. 41th IEEE Conf. on Decision and Control, 2002, pp. 1552–1557.
[36] C. Kirches, *A Numerical Method for Nonlinear Robust Optimal Control with Implicit Discontinuities and an Application to Powertrain Oscillations*, Diploma Thesis, Heidelberg University, October 2006.
[37] C. Kirches and F. Lenders, *Approximation properties and tight bounds for constrained mixed-integer optimal control*, Optimization Online (2016), (submitted to Mathematical Programming).
[38] C. Kirches, A. Potschka, H.G. Bock, and S. Sager, *A Parametric Active Set Method for a Subclass of Quadratic Programs with Vanishing Constraints*, Pacific Journal of Optimization **9** (2013), no. 2, 275–299.
[39] R. I. Leine, D. H. Van Campen, and B. L. Van De Vrande, *Bifurcations in nonlinear discontinuous systems*, Nonlinear Dynamics **23** (2000), no. 2, 105–164.
[40] R.I. Leine, *Bifurcations in discontinuous mechanical systems of filippov-type*, PhD thesis, Techn. Univ. Eindhoven, The Netherlands, 2000.
[41] R.I. Leine, D.H. van Campen, A. de Kraker, and L. van den Steen, *Stick-slip vibrations induced by alternate friction models*, Nonlinear Dynamics **16** (1998), no. 1, 41–54.
[42] R.C. Loxton, K.L. Teo, and V. Rehbock, *Optimal control problems with multiple characteristic time points in the objective and constraints*, Automatica **44** (2008), no. 11, 2923 – 2929.
[43] O.L. Mangasarian and S. Fromovitz, *Fritz John necessary optimality conditions in the presence of equality and inequality constraints*, Journal of Mathematical Analysis and Applications **17** (1967), 37–47.
[44] R.B. Martin, *Optimal control drug scheduling of cancer chemotherapy*, Automatica **28** (1992), no. 6,

1113 – 1123.

[45] M.J. Mohideen, J.D. Perkins, and E.N. Pistikopoulos, *Towards an efficient numerical procedure for mixed integer optimal control*, Computers & Chemical Engineering **21** (1997), S457–S462.

[46] K.D. Mombaur, *Stability Optimization of Open-loop Controlled Walking Robots*, Ph.D. thesis, Universität Heidelberg, 2001.

[47] B. Piccoli, *Necessary conditions for hybrid optimization*, Decision and Control, 1999. Proceedings of the 38th IEEE Conference on, vol. 1, 1999, pp. 410–415 vol.1.

[48] R. Raman and I. E. Grossmann, *Modelling and computational techniques for logic based integer programming*, Computers and Chemical Engineering **18** (1994), no. 7, 563–578.

[49] J. Roll, *Identification of piecewise affine systems via mixed-integer programming*, Automatica **40** (2004), no. 1, 37–50.

[50] A. Saccon, N.V.D. Wouw, and H. Nijmeijer, *Sensitivity analysis of hybrid systems with state jumps with application to trajectory tracking*, IEEE Conference on Decision and Control (2014), no. 27, 3065–3070.

[51] S. Sager, *Numerical methods for mixed–integer optimal control problems*, Ph.D. thesis, Universität Heidelberg, 2006.

[52] S. Sager, H.G. Bock, and M. Diehl, *The Integer Approximation Error in Mixed-Integer Optimal Control*, Mathematical Programming A **133** (2012), no. 1–2, 1–23.

[53] S. Sager, G. Reinelt, and H.G. Bock, *Direct Methods With Maximal Lower Bound for Mixed-Integer Optimal Control Problems*, Mathematical Programming **118** (2009), no. 1, 109–149.

[54] S. Scholtes, *Convergence properties of a regularization scheme for mathematical programs with complementarity constraints*, SIAM Journal on Optimization **11** (2001), 918–936.

[55] O. von Stryk and M. Glocker, *Decomposition of Mixed-Integer Optimal Control Problems Using Branch and Bound and Sparse Direct Collocation*, Proc. ADPM 2000 – The 4th International Conference on Automatisation of Mixed Processes: Hybrid Dynamical Systems, 2000, pp. 99–104.

[56] H.J. Sussmann, *A maximum principle for hybrid optimal control problems*, Conference proceedings of the 38th IEEE Conference on Decision and Control (Phoenix), 1999.

[57] P. Tabuada, *Verification and control of hybrid systems: a symbolic approach*, Springer Science & Business Media, 2009.

[58] S. Wei, K. Uthaichana, M. Žefran, R.A. DeCarlo, and S. Bengea, *Applications of numerical optimal control to nonlinear hybrid systems*, Nonlinear Analysis: Hybrid Systems **1** (2007), no. 2, 264–279.

[59] S.F. Woon, V. Rehbock, and R. Loxton, *Towards global solutions of optimal discrete-valued control problems*, Optimal Control Applications and Methods **33** (2012), no. 5, 576–594.

[60] X. Xu and P.J. Antsaklis, *Results and Perspectives on Computational Methods for Optimal Control of Switched Systems*, pp. 540–555, Springer Berlin Heidelberg, Berlin, Heidelberg, 2003.

[61] ———, *Optimal control of switched systems based on parameterization of the switching instants*, IEEE Transactions on Automatic Control **49** (2004), no. 1, 2–16.

[62] F. Zhu and P.J. Antsaklis, *Optimal control of hybrid switched systems: A brief survey*, Discrete Event Dynamic Systems **25** (2015), no. 3, 345–364.